Pixel-Level Synergy: Merging Euclid and LSST/Rubin for Precision Cosmology

Jean-Luc Starck

http://jstarck.cosmostat.org

Collaborators: **Utsav Akhaury (EPFL), Pascale Jablonka (EPFL), Frederic Courbin (ICREA, Spain)**

COSMOSTAT

TITAN

Artificial Intelligence in Astrophysics

www.cosmostat.org

Motivations

-**Euclid:**

- High resolution: good for galaxies detection and shape measurement.
- Need extra colors for redshift estimation.

Rubin:

- More bands
- Lower resolution (blending of galaxies, etc)

Ideally, we would like to have a **Joint Euclid-Rubin (JEUBIN Catalog),** using both **Euclid resolution** and **Rubin colours.**

➡**Part 1: Introduction**

➡**Part 2: Ground Based Telescope PSF**

➡**Part 3: Space Telescope PSF**

➡**Part 4: Joint Rubin-Euclid Deconvolution**

Large Field Image Deconvolution

Deconvolution

$$Y = HX + N$$

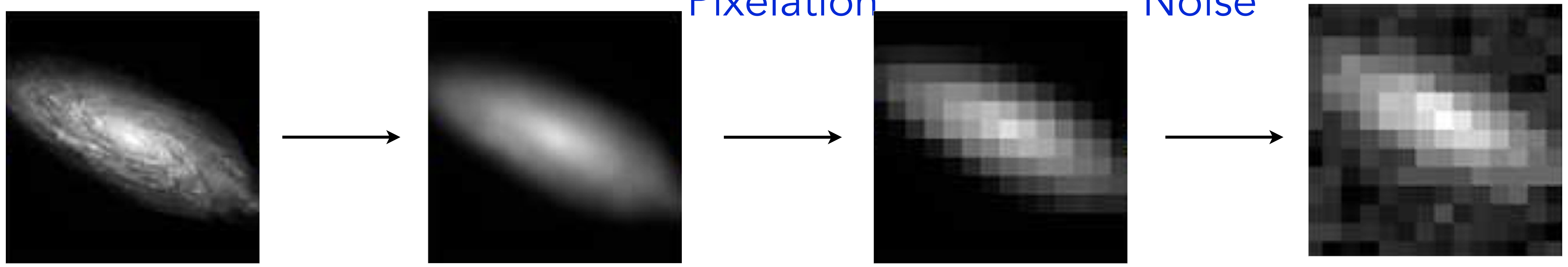

Ground: Subaru (8.2m) Space: HST (2.4m)

Euclid Space Variant Point Spread Function

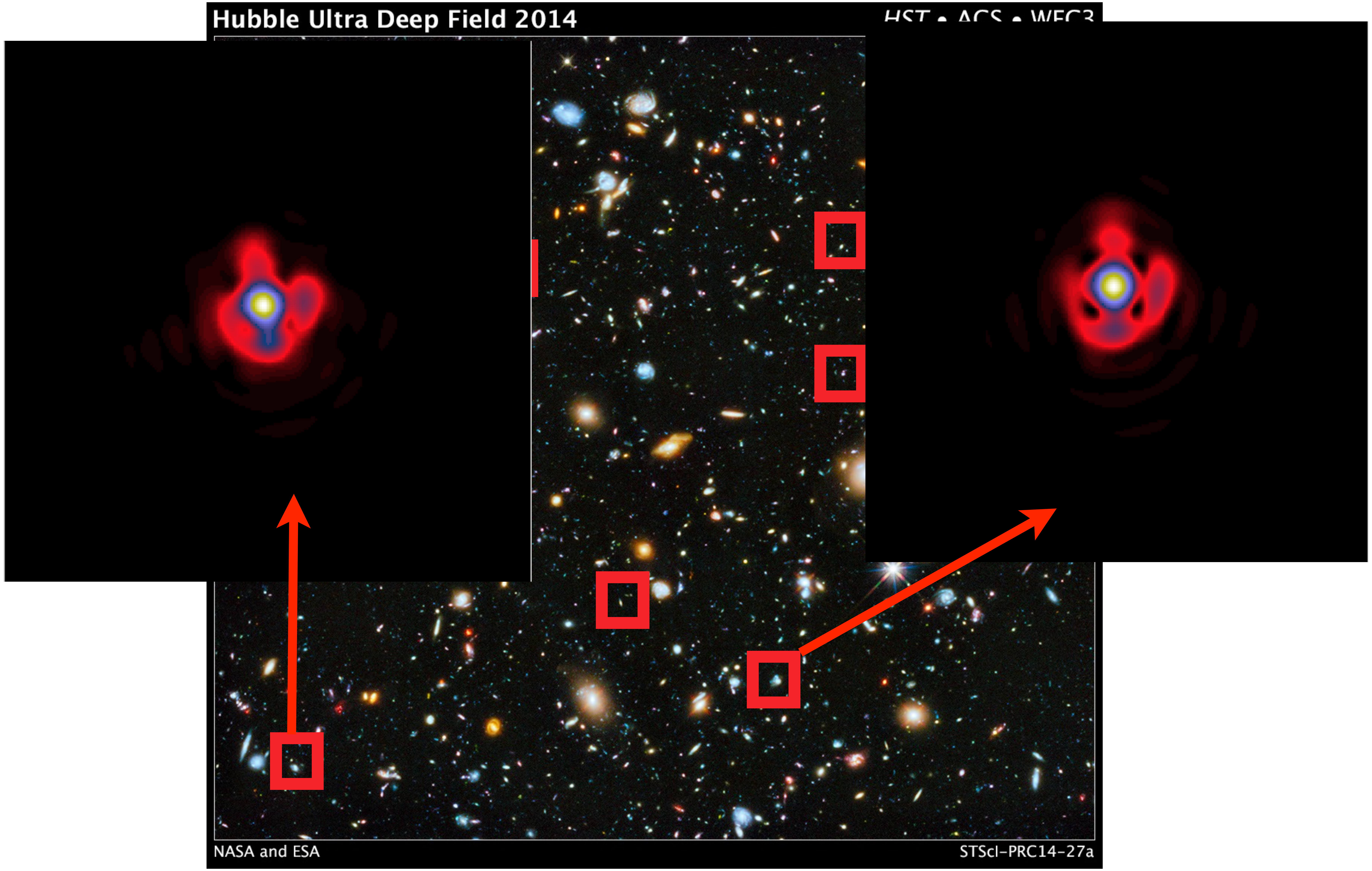

Galaxies Survey Image Deconvolution

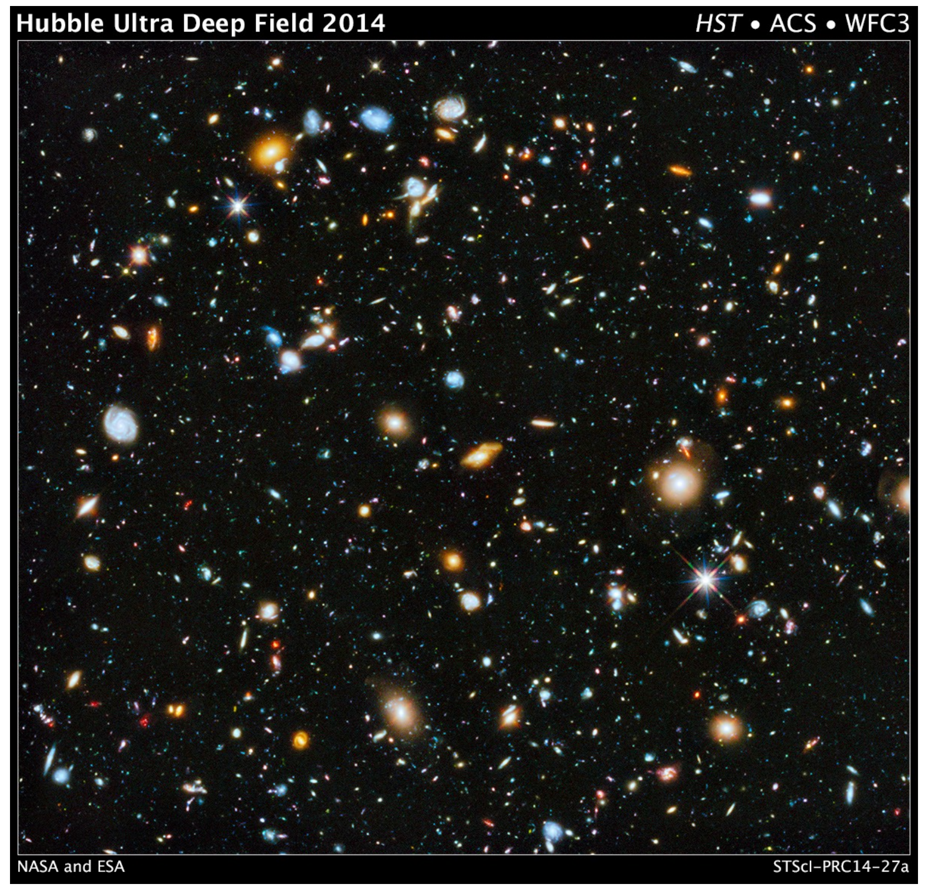

Sandard deconvolution framework:

$$\mathbf{y} = \mathbf{H}\mathbf{x} + \mathbf{n}$$

Noise
True Image
PSF Convolution
Observed Image

Sandard deconvolution framework:

$$\underset{\mathbf{X}}{\operatorname{argmin}} \quad \frac{1}{2}\|\mathbf{Y} - \mathbf{H}\mathbf{X}\|_2^2$$

H is huge !!!

Detection + Classification stars/galaxies

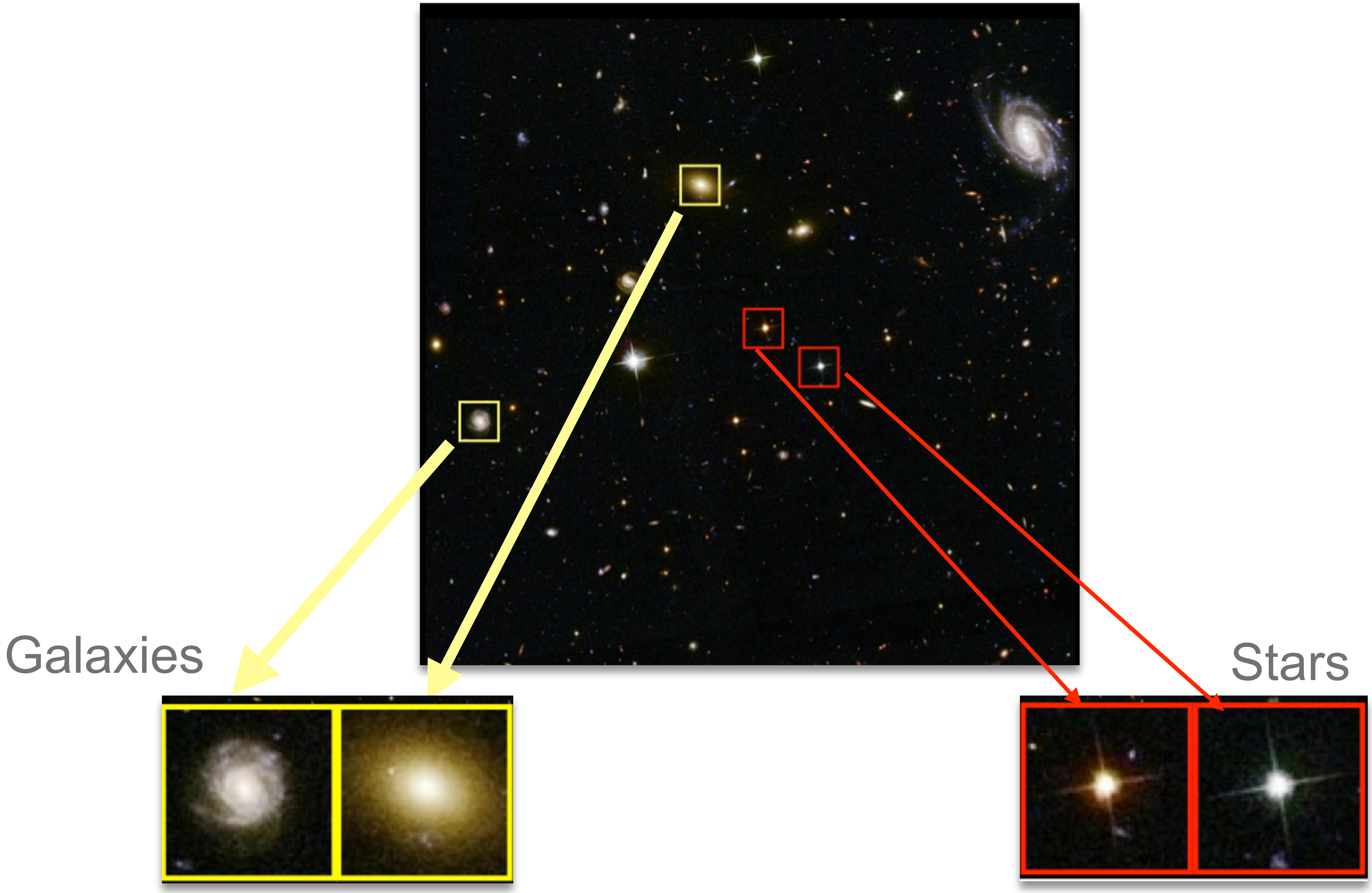

An Inverse Problem

The deconvolution problem $y = hx + n$ Least Square estimator $\| y - hx \|^2$

But there is no unique and stable solution, it is an ill posed inverse problem.

$$\| y - hx \|^2 + \mathcal{C}(x)$$

Physical Knowledge on X (ex: Gaussian Random Field, etc).
==> Gaussian smoothing, Wiener reconstruction, etc
==> Log normal distribution prior

X properties are understood through a representative data set
==> X Learning, X in (Dictionary, Machine, Deep)

Knowledge on the histogram of X in pixel space or in another one.
==> Positivity constraint, sparsity constraint, etc.

Convolution Operator + Sampling

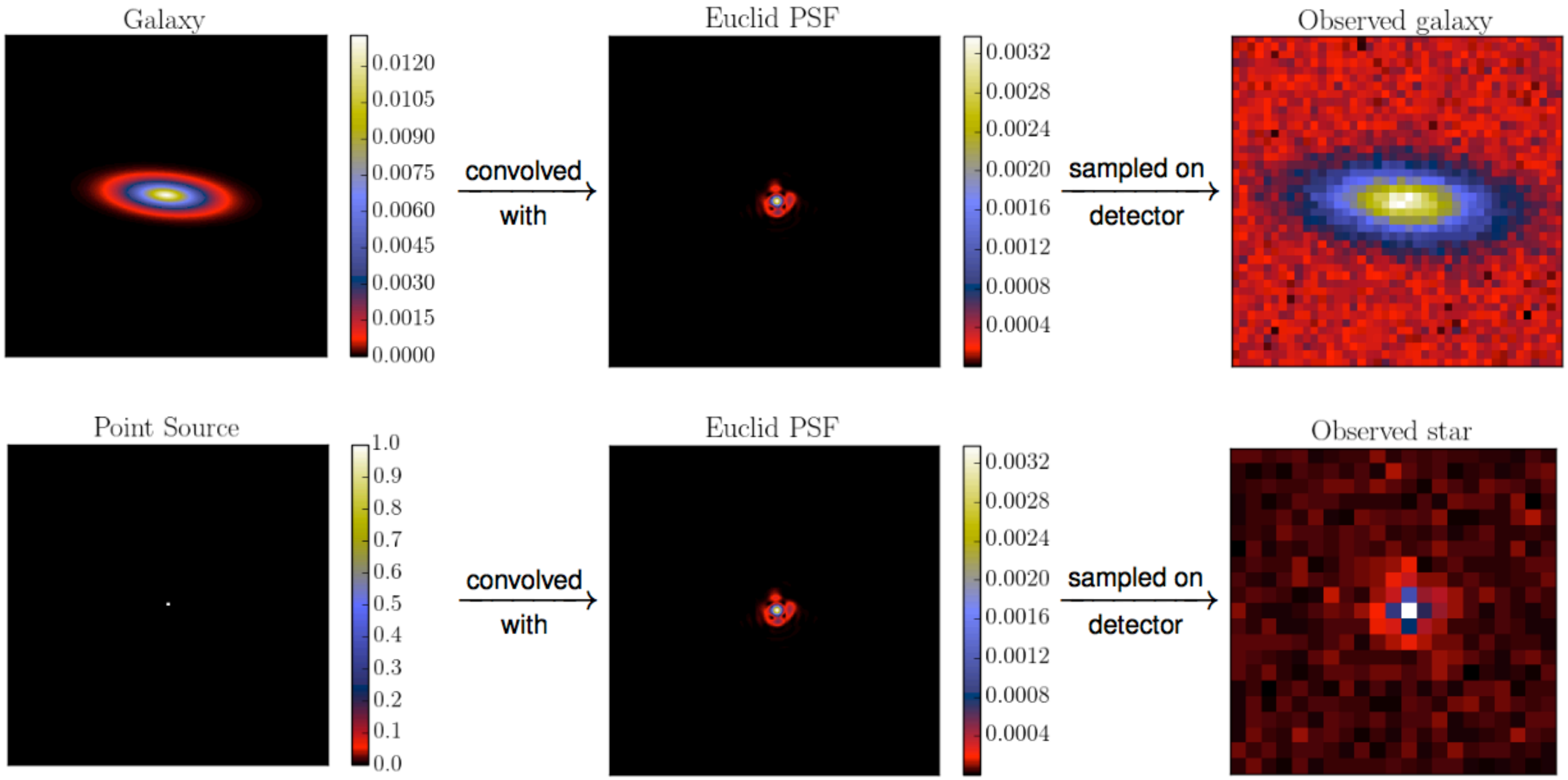

The PSF Challenge

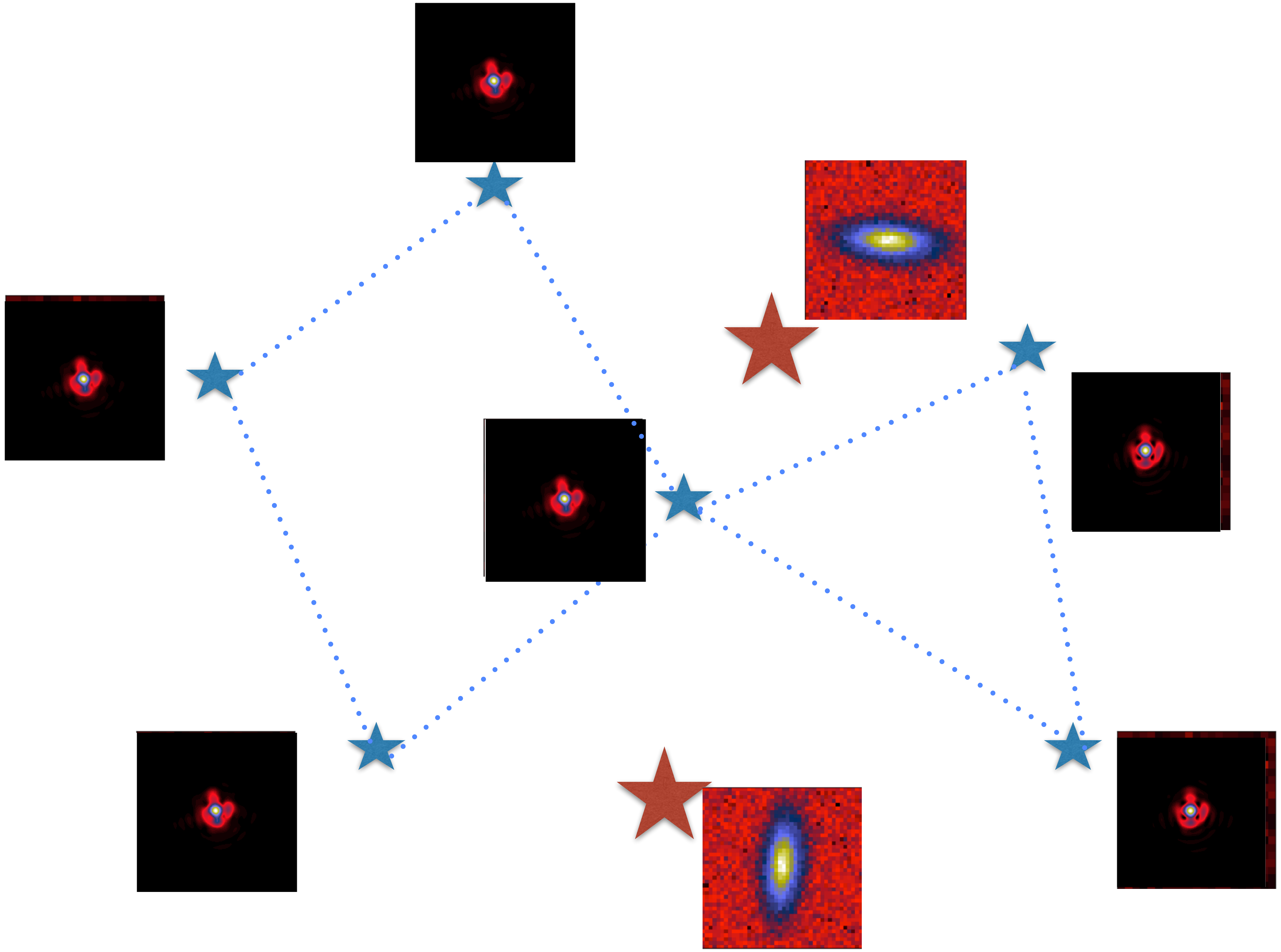

➡**Part 1: Introduction**

➡**Part 2: Ground Based Telescope PSF**

➡**Part 3: Space Telescope PSF**

➡**Part 4: Joint Rubin-Euclid Deconvolution**

PSF Recovery

PSFEx: Models the **point spread function (PSF)** from observed stars, adjusting its spatial variation across the field to correct for instrumental and atmospheric effects.

Lensfit: Performs **Bayesian galaxy shape estimation** by fitting PSF-convolved galaxy models.

MCCD (Liaudat et al. , A&A 646, A27 (2021)): Modelling the full PSF field.

The PSF Field Recovery Problem

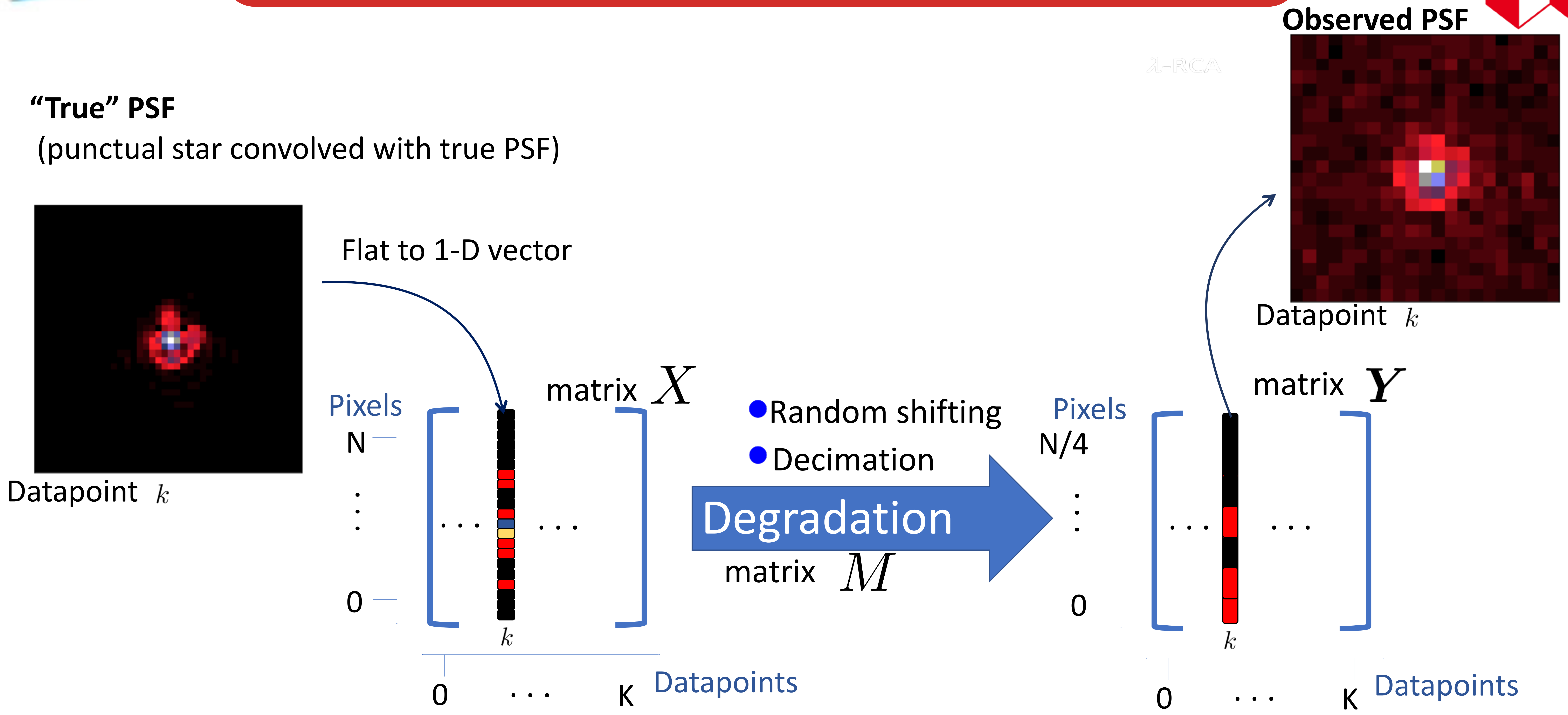

$$\min_{X} \| Y - MX \|^2$$

- $X \in \mathbb{R}_+^{N \times K}$: true PSFs at different positions of the FOV.
- $\boldsymbol{M} = [\boldsymbol{M}_1, \cdots, \boldsymbol{M}_K],\ \boldsymbol{M}_k \in \mathbb{R}_+^{N' \times N}$: decimation and shifting.
- $\boldsymbol{Y} \in \mathbb{R}_+^{N' \times K}$: observed PSFs.

Constraints

Joint estimations of super-resolved PSFs at stars positions

➡ Low rank constraint: Constraint the PSFs to be a linear combination of the ***eigenvectors*** PSFs:

$$\mathbf{PSF}^{(k)} = x_k = \sum_{i=1}^{r} a_{i,k} s_i$$

s_i = ith *vector* (2D image)

$a_{i,k}$ = coefficient corresponding to contribution of the i-th vector to the k-th PSF.

Eigen PSF

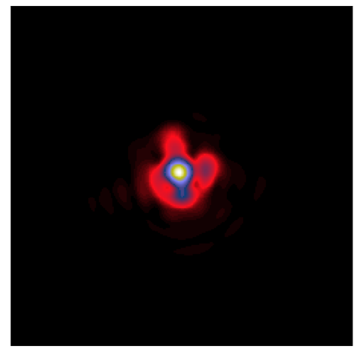

➡ Positivity constraint (**$x_k > 0$**)

➡ Smoothness constraint on each s_i $\sum_r \| \Phi s_i \|_1$

➡ Proximity constraint on the $a_{i,k}$ coefficients: the closer are the stars, the more the coefficients of the linear combination ar

$u_i \in \mathcal{U}_{\text{stars}}$

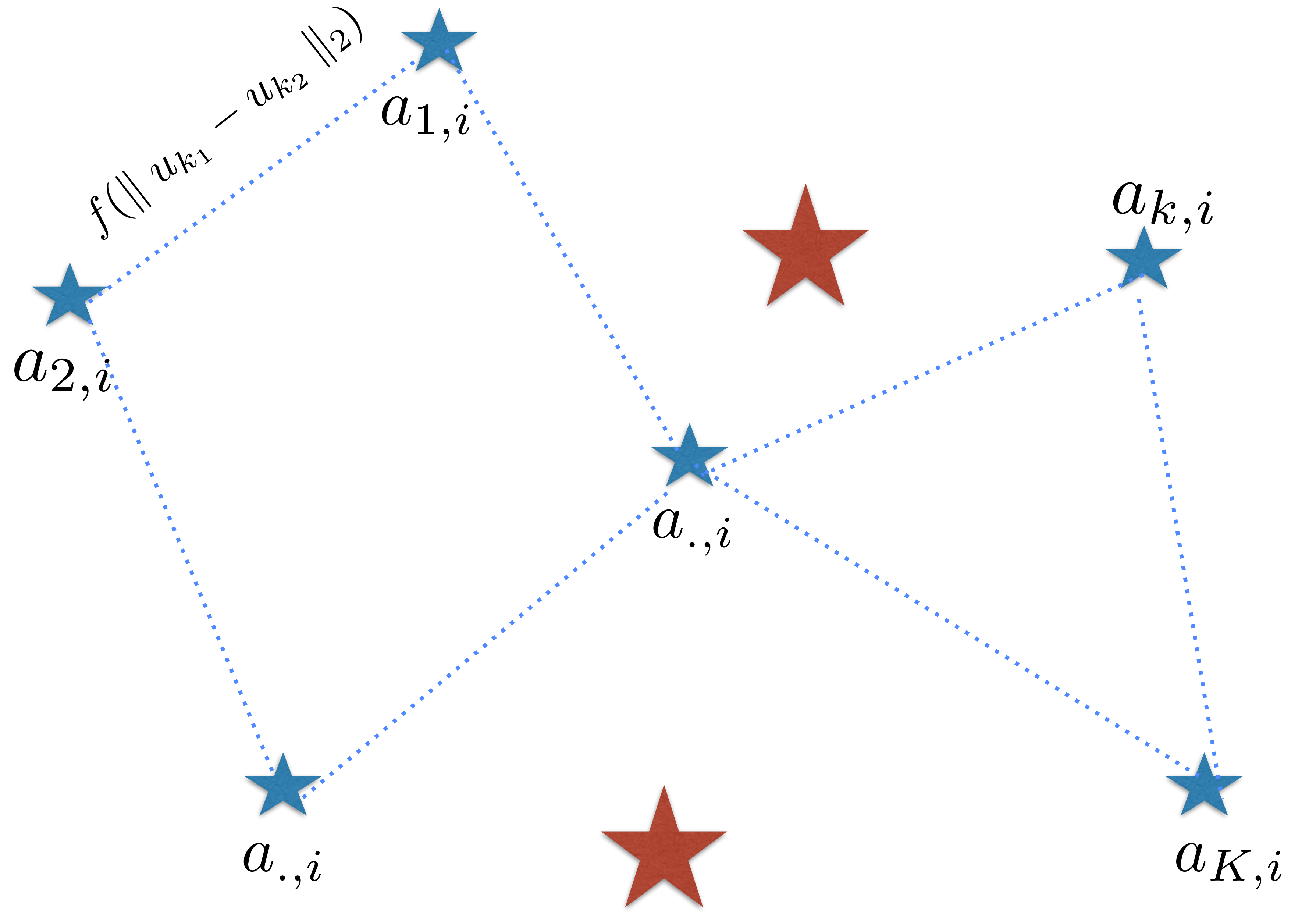

PSF Laplacian Graph

Laplacian Graph **P = D - A**,   where D is the degree matrix and A is the adjacent matrix of the graph

$$P^t P = V \Lambda V^t$$

- Degree matrix= diagonal matrix with information about the degree of each vertex—that is, the number of edges attached to each vertex.
- Adjacent matrix A: element Air is one when there is an edge from vertex i to vertex j, and zero when there is no edge.

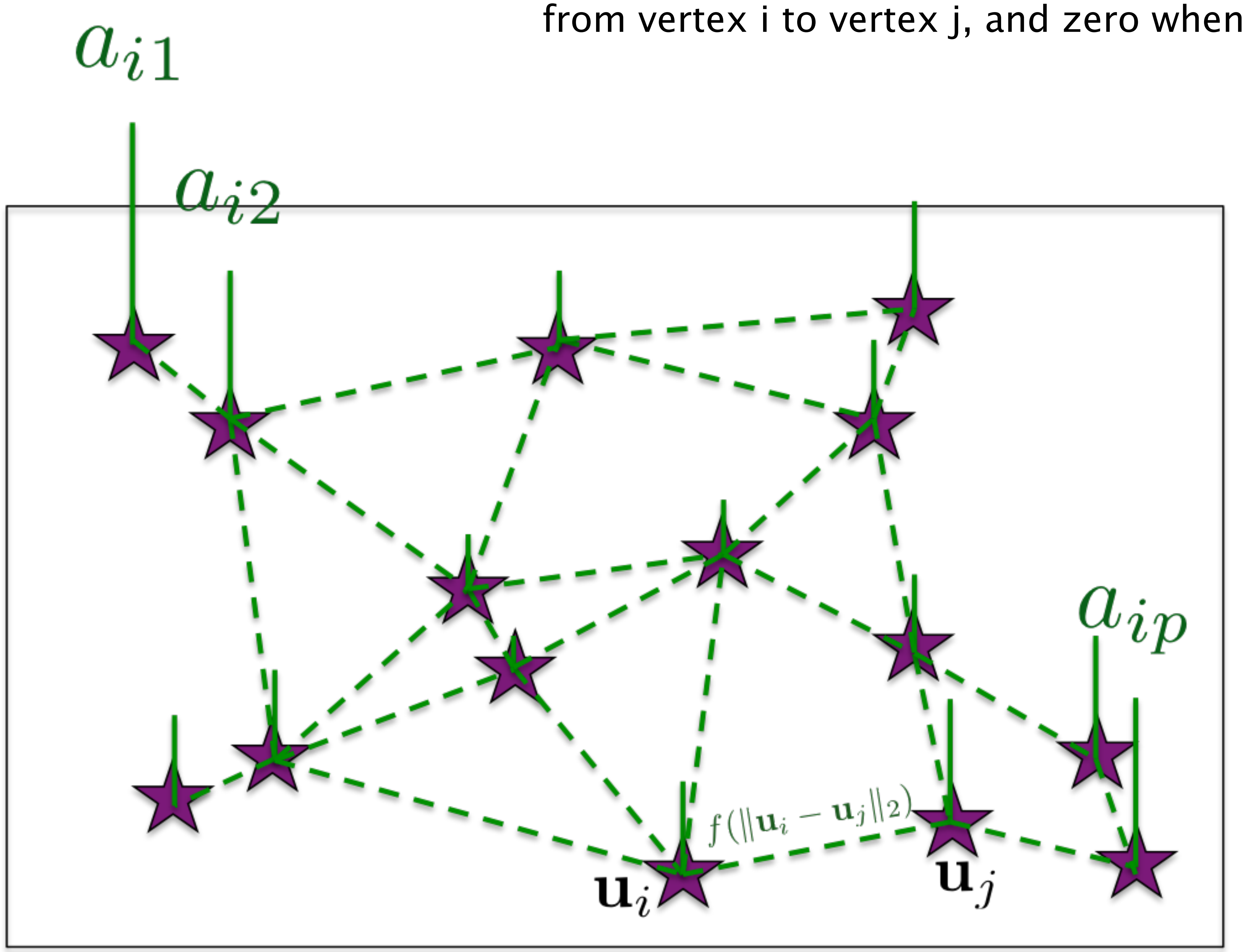

Matrix Factorization

MODEL: $\mathbf{X}$ $\mathbf{S}$ $\mathbf{A}$

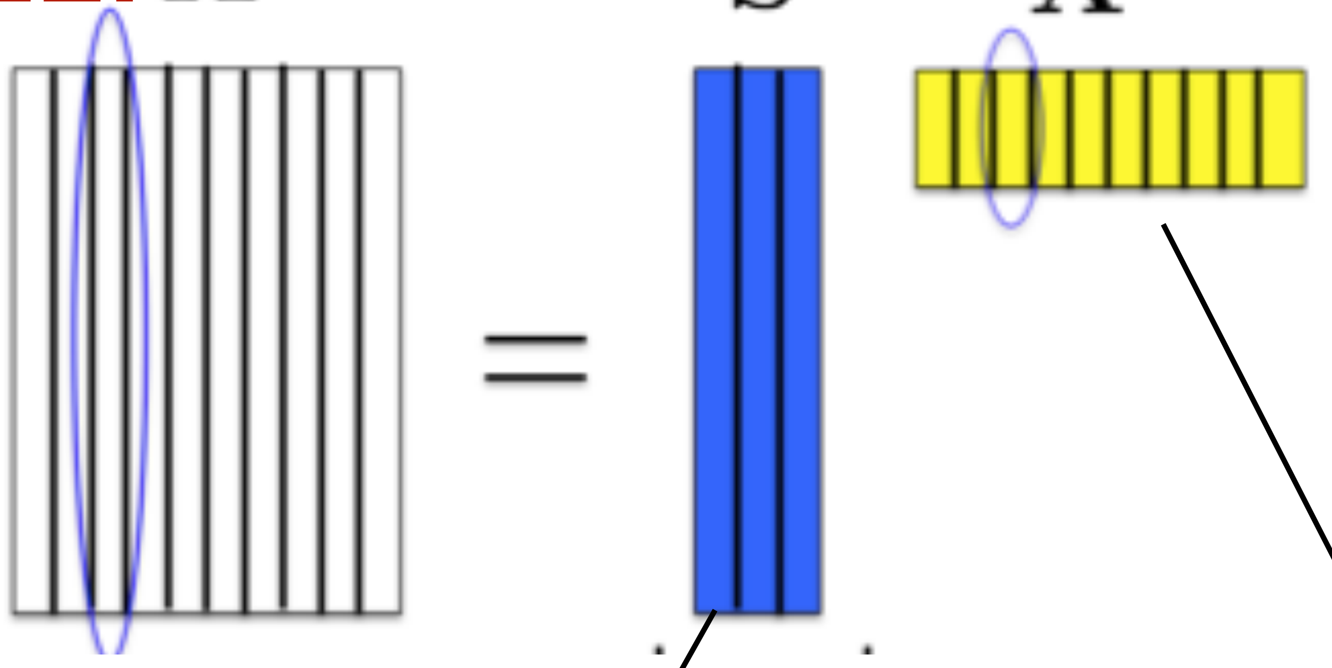

$$\mathbf{S} = [\mathbf{s}_1, \ldots, \mathbf{s}_p]$$

$$\mathbf{PSF}^{(k)} = x_k = \sum_{i=1}^{r} a_{i,k} s_i$$

s_i are "eigen PSF"

$$A = \alpha V^\top$$

Each eigen PSF is sparse in a wavelet dictionary

$$\sum_r \| \Phi s_i \|_1$$

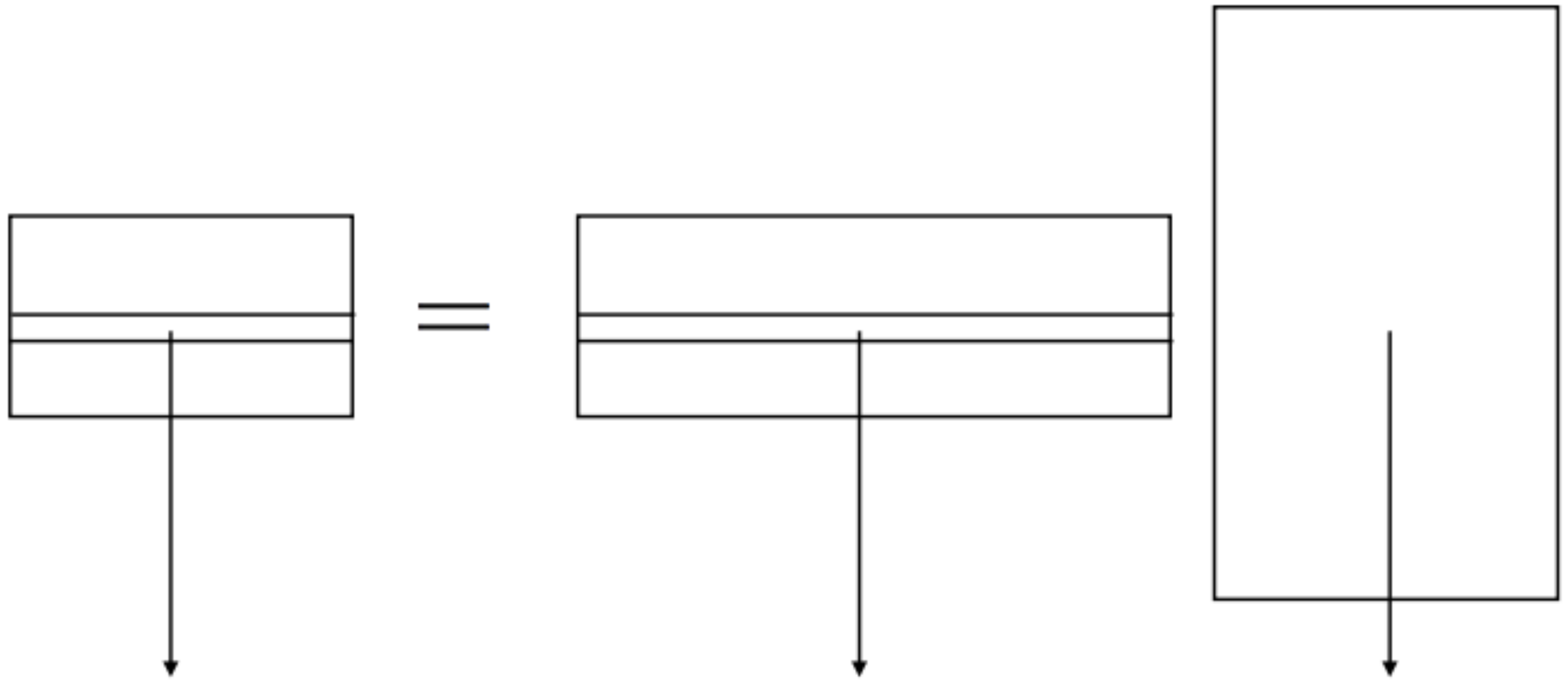

A_i: function on PSF graph associated with eigenPSF S_i

α_i: sparse to enforce spatial constraints

Eigenvectors of PSF graphs' Laplacians

http://www.cosmostat.org/software/rca/

Matrix Factorization

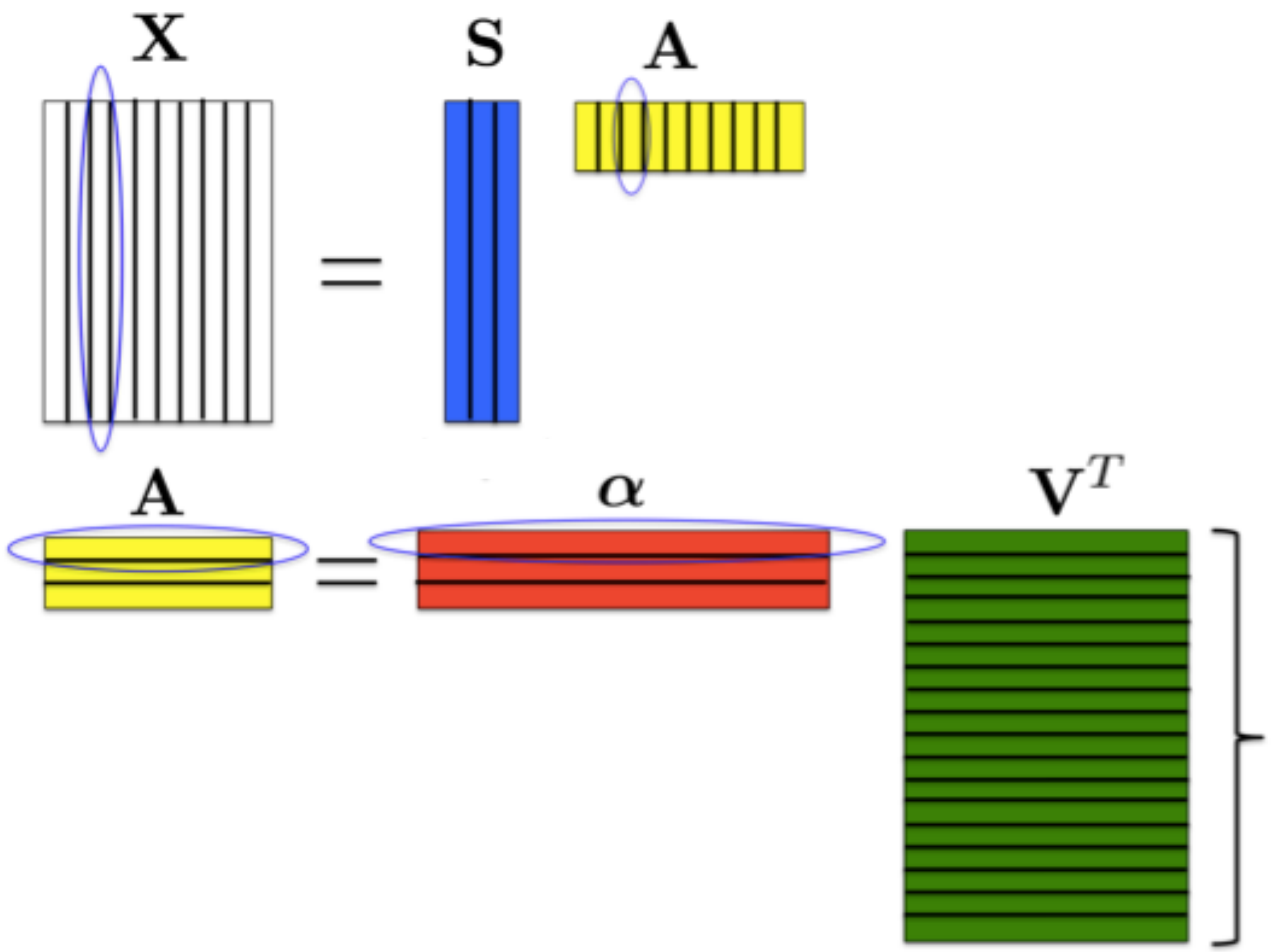

$$\min_{S,\alpha} \frac{1}{2}\|Y - M(S\alpha V^\top)\|_2^2 + \sum_{i=1}^{r} \|w_i \odot \Phi s_i\|_1 + \iota_+(S\alpha V^\top) + \iota_\Omega(\alpha)$$

Data fidelity term

Sparsity on the eigen PSF: the PSF should have a sparse representation in an appropriate basis

Positivity Constraint

Smoothness of the PSF field constraint : the smaller the difference between two PSFs' positions u_i , u_j , the smaller the difference between their estimated representations

http://www.cosmostat.org/software/rca/

Numerical Experiments

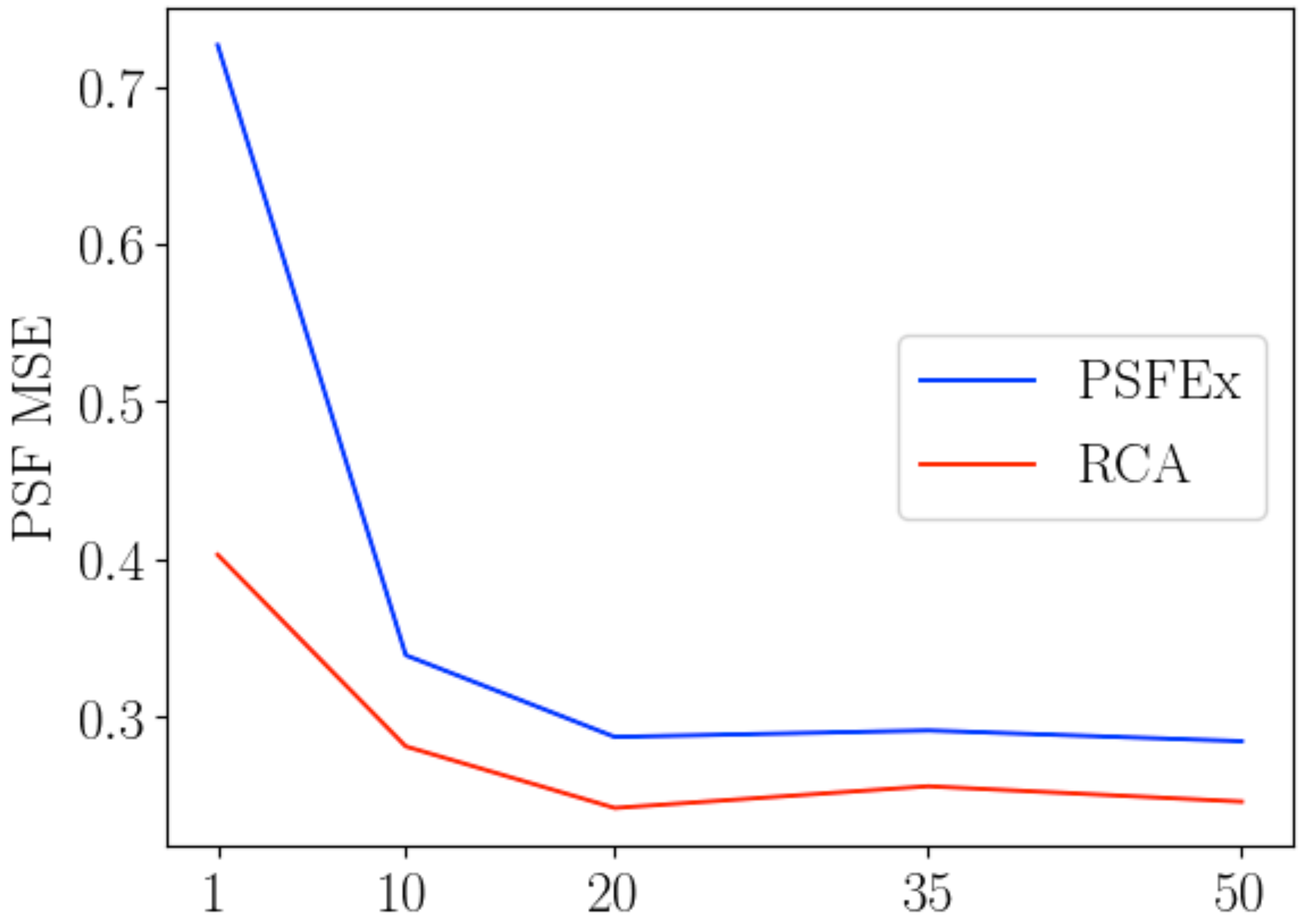

Stars SNR

Multi-CCD PSF model

Tobias Liaudat

Liaudat et al. , A&A 646, A27 (2021)

https://github.com/CosmoStat/mccd

$$\hat{H}_k = \underbrace{S_k \, A_k}_{\text{Local: } \hat{H}_k^{\text{Loc}}} + \underbrace{\tilde{S} \, \tilde{A}_k}_{\text{Global: } \hat{H}_k^{\text{Glob}}}$$

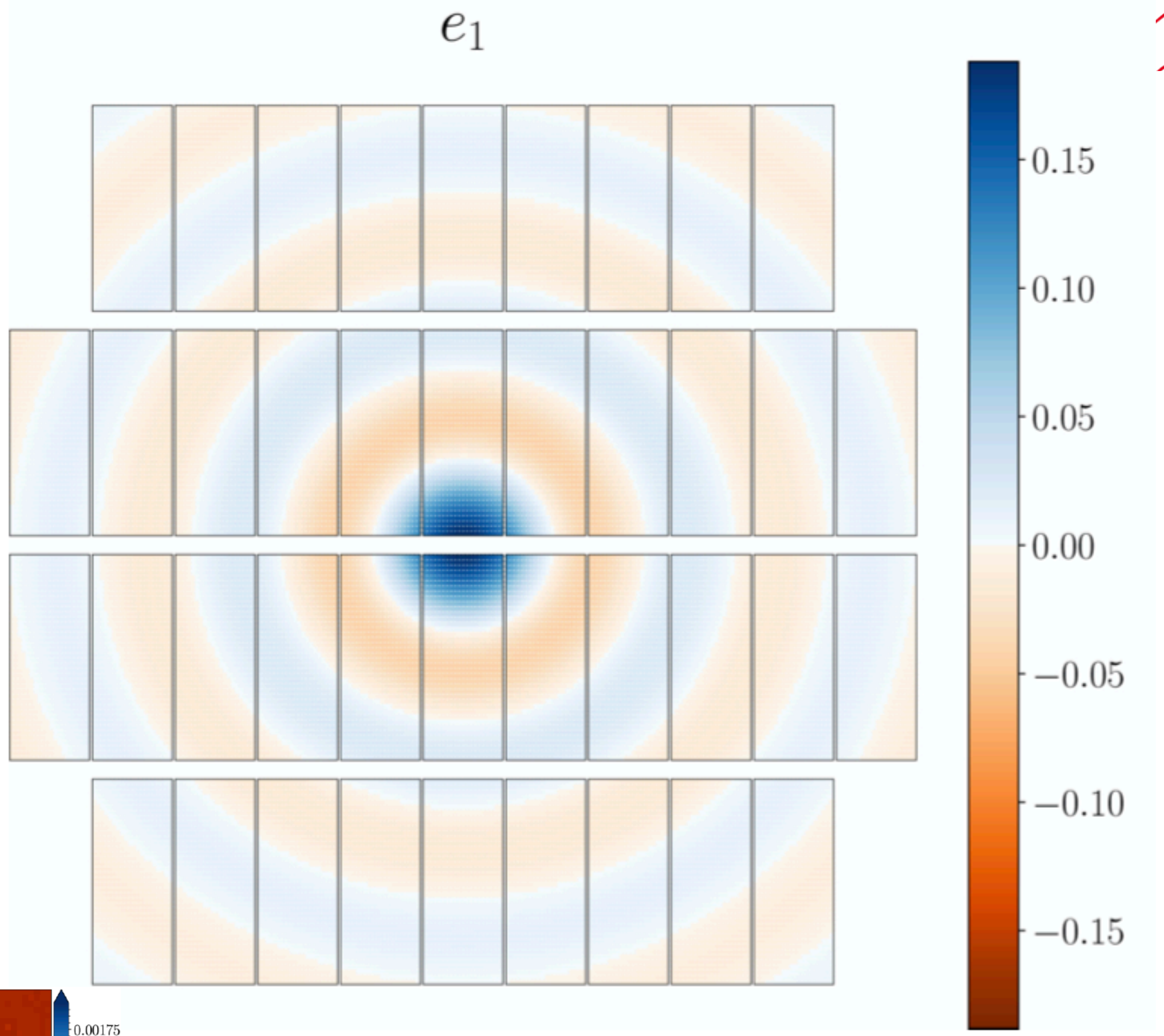

$\hat{H}_k$: **PSF reconstructions for CCD** k

$\tilde{S}$: **global PSF features**

S_k : **local PSF features**

$\tilde{A}_k$: **global features weights**

A_k : **local features weights**

Common to all CCDs

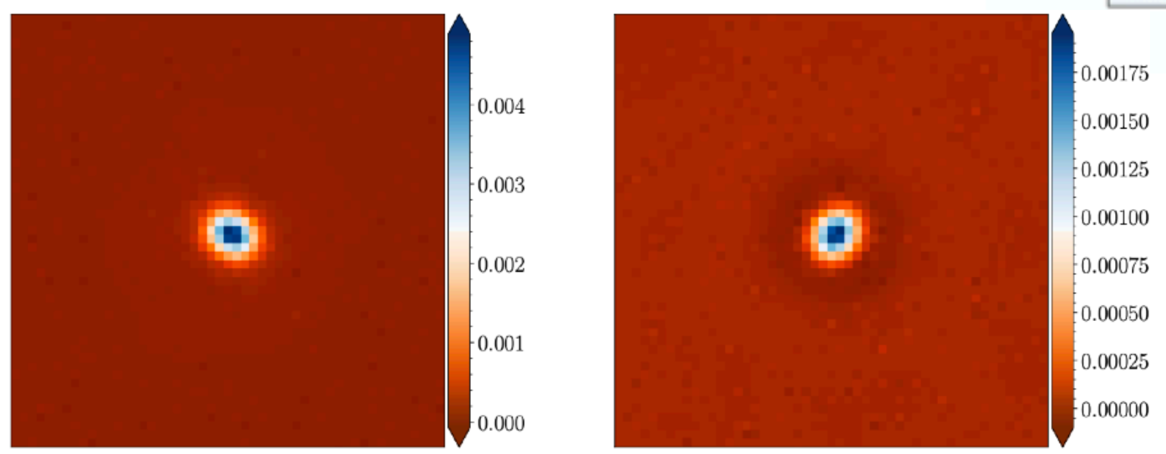

CCD-specific

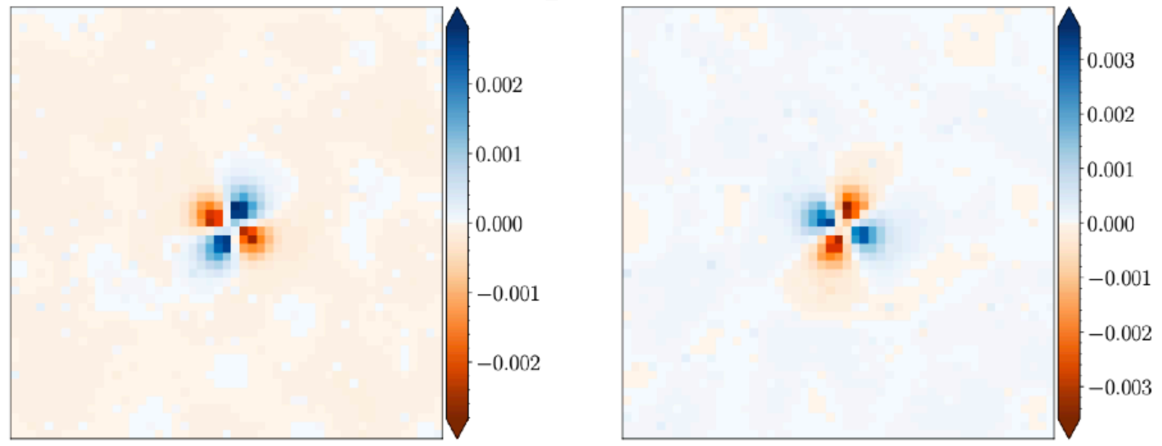

Numerical Experiments

Tobias Liaudat

- **Qp1 : Pixel RMSE taking into consideration the noise level**
- **Qp2 : Mean standard deviation of model's noise**
- **Qp3 : Variation of model's noise over Qp2**

CFIS Real Data

Method	Q_{p_1}	Q_{p_2}	Q_{p_3}
PSFEx	15.56	8.13	14.31
MCCD-HYB	**12.14**	**6.68**	**10.86**
$\text{Gain}_{\text{PSFEx}}$	22%	18%	24%

Model's reconstruction error

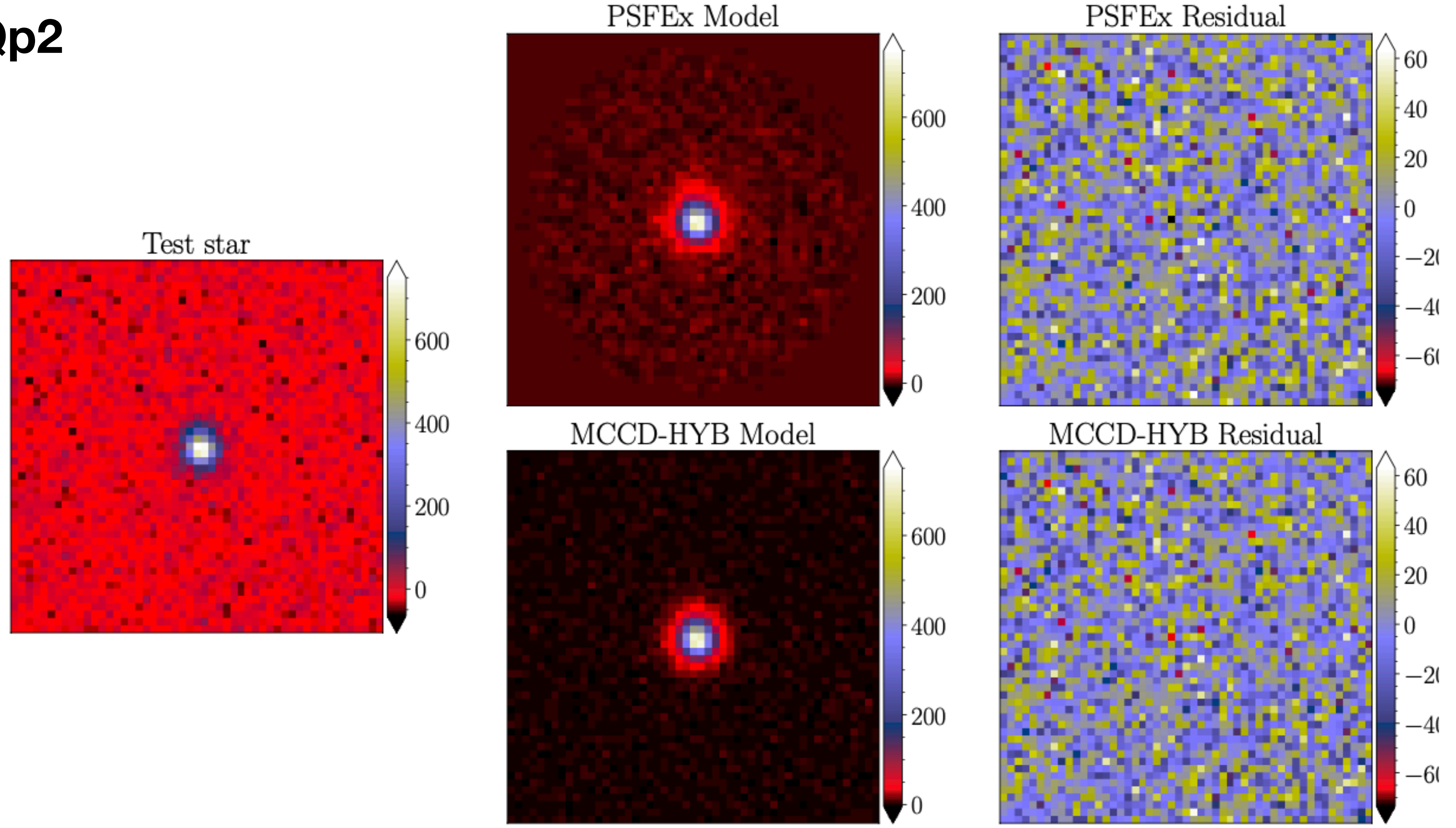

$$\min_{S,\alpha} \frac{1}{2}\|Y - M(S\alpha V^\top)\|_2^2 + \sum_{i=1}^{r} \|w_i \odot \Phi s_i\|_1 + \iota_+(S\alpha V^\top) + \iota_\Omega(\alpha)$$

- T. Liaudat et al, "Multi-CCD Point Spread Function Modelling", **Astronomy and Astrophysics**, 646, id.A27, 18 pp, 2021.

➡**Part 1: Introduction**

➡**Part 2: Ground Based Telescope PSF**

➡**Part 3: Space Telescope PSF**

➡**Part 4: Joint Rubin-Euclid Deconvolution**

Euclid PSF Modeling

- PSF Modeling
  - ➡Undersampling
  - ➡Space dependency
  - ➡ Time dependency
  - ➡Wavelength dependency
  - ➡Multi-CCD

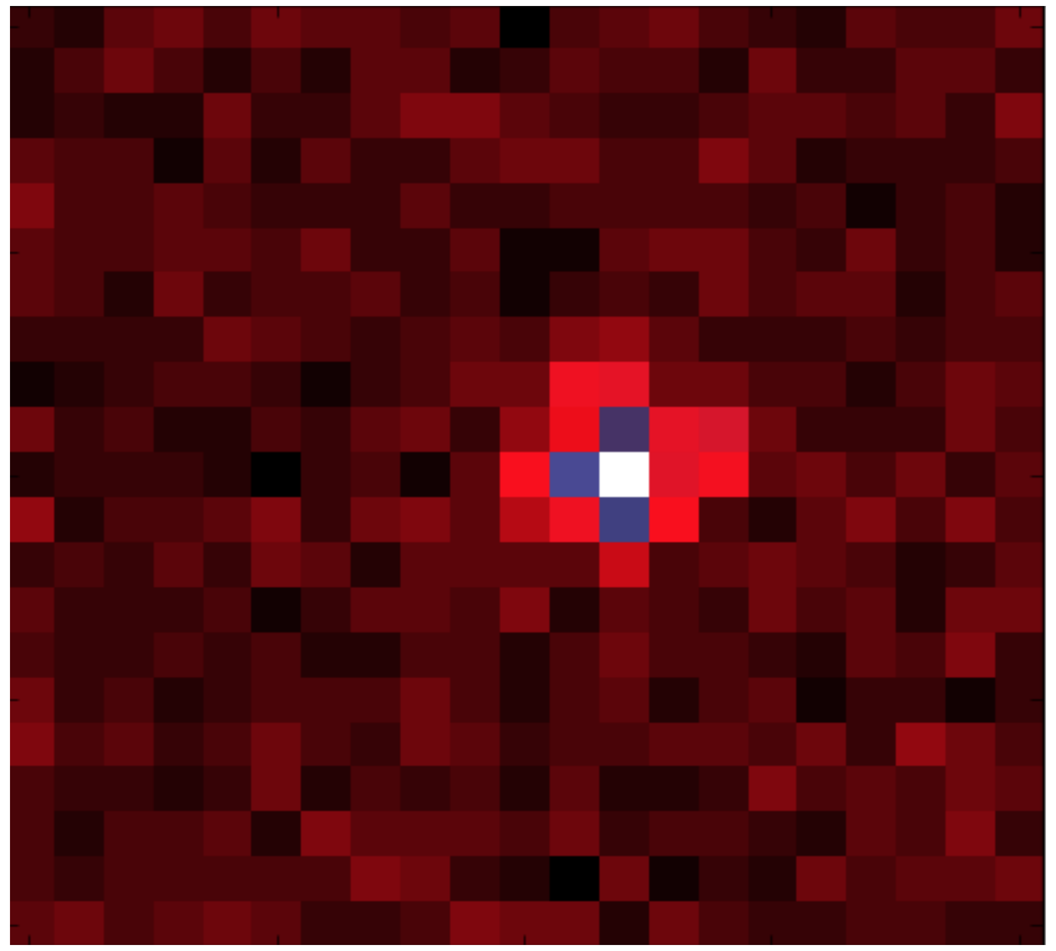

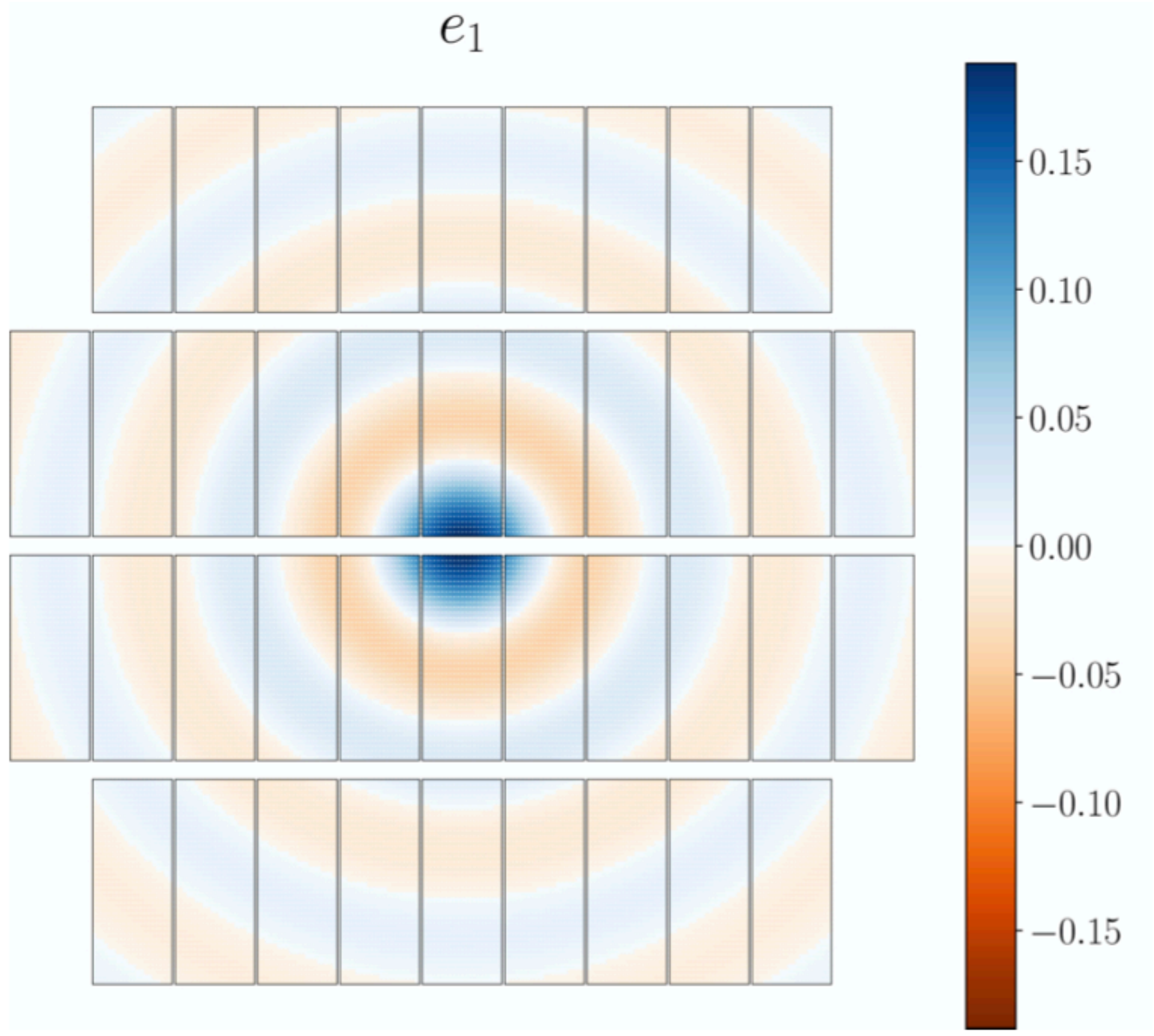

Wave Front Error (WFE) modelling

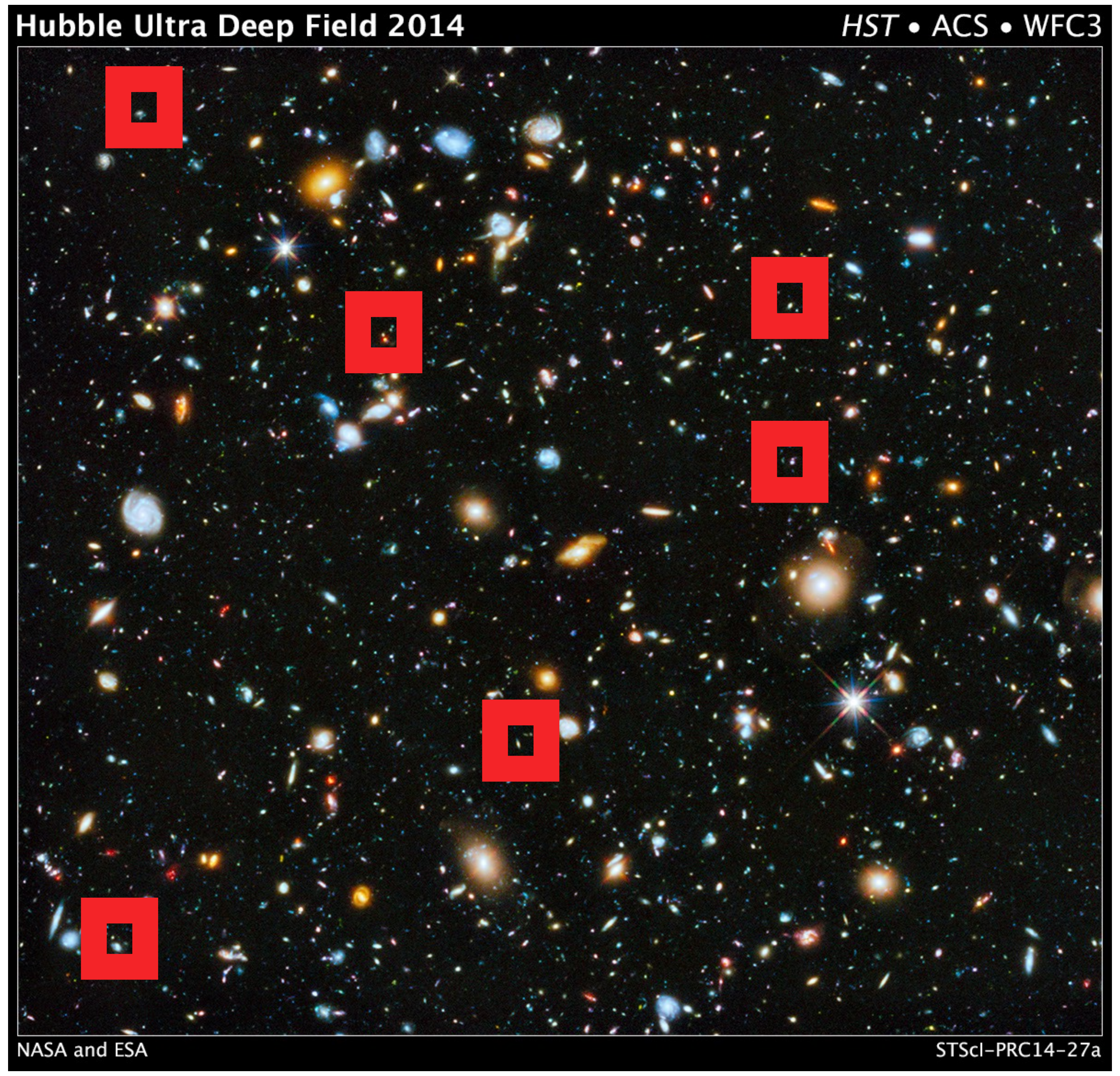

Star observation

$$\bar{\mathcal{H}}_{u_i} \approx \sum_{b=1}^{N_\lambda} S_{u_i}(\lambda_b)\ \mathcal{H}_{u_i}^{\lambda_b}$$

- Star considered as point source
- Discretization of the integral into N wavelength bins
- Star SED information known

Objective

From a set of $\bar{\mathcal{H}}_{u_i}$ and $S_u(\lambda)$ we need to estimate $\mathcal{H}_u^\lambda$ at any position and wavelength.

Euclid PSF Modeling

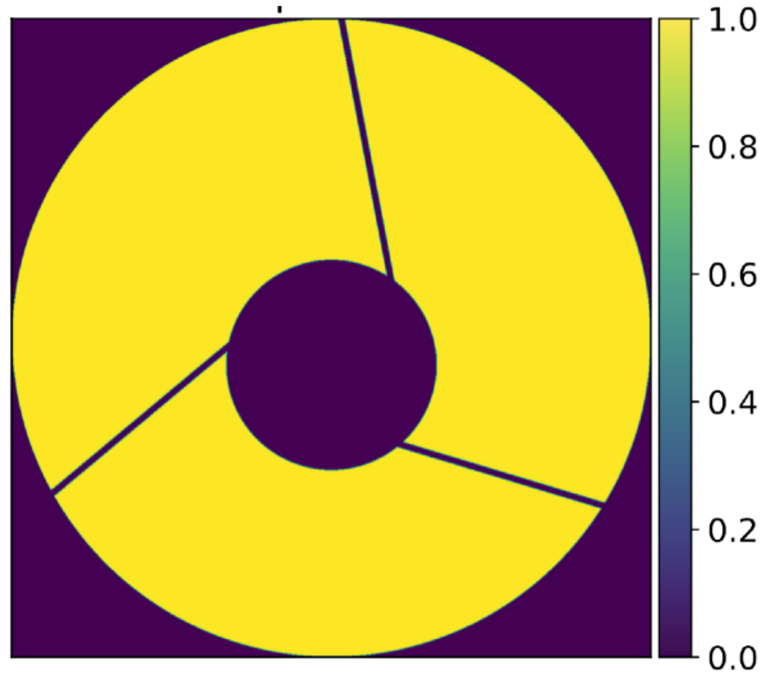

$$\underbrace{\hat{\mathcal{H}}_{u_i}^{\lambda}}_{\text{Monochromatic PSF reconstruction}} \propto \underbrace{\mathcal{D}_{\theta}}_{\text{Diffraction operator + Downsampling}} \left\{ \underbrace{P_{u_i}^{\lambda}}_{\text{Obscurations}} \odot \exp \left[2\pi i \left(\underbrace{\frac{\Phi_{u_i}}{\lambda}}_{\text{WFE Parametric Component}} \right) \right] \right\}$$

Star observation

$$\bar{\mathcal{H}}_{u_i} \approx \sum_{b=1}^{N_\lambda} S_{u_i}(\lambda_b)\, \mathcal{H}_{u_i}^{\lambda_b}$$

- Star considered as point source
- Discretization of the integral into N wavelength bins
- **Star SED information known**

Wavefront Error Modeling

Tobias Liaudat

- The model is now build on the wavefront error (WFE) and not on the pixel images.

WFE = Parametric Part +   Non Parametric Part

- The non parametric to correct **the mismatch** between the model and the truth.
- Easier include the **dichroic coating effect.**
- **RCA regularization** technique on the Non Parametric Part.

GPU + TensorFlow automatic differentiation

- Uses a forward model, WFE → pixels
  - Includes diffraction phenomena, obscuration, downsampling, etc..
- **End-to-end differentiable!**
  - Based on an automatic differentiation framework → TensorFlow.
  - Fast computations on GPU.

Euclid Point Spread Function Field

Forward model

$$\hat{\mathcal{H}}^{\lambda}_{u_i} \propto \mathcal{D}_{\theta} \left\{ P^{\lambda}_{u_i} \odot \exp\left[2\pi i \left(\frac{\Phi_{u_i}}{\lambda} + C^{\lambda}_{u_i} \right) \right] \right\}$$

$$\bar{\mathcal{H}}_{u_i} \approx \sum_{b=1}^{N_{\lambda}} S_{u_i}(\lambda_b)\, \mathcal{H}^{\lambda_b}_{u_i}$$

Monochromatic PSF reconstruction

Diffraction operator + Downsampling

$$\approx \mathrm{crop}_N \left\{ \left| \mathrm{FFT}\left[\mathrm{pad}_{N_{\mathrm{FFT}}}(\cdot) \right] \right|^2 \right\}$$

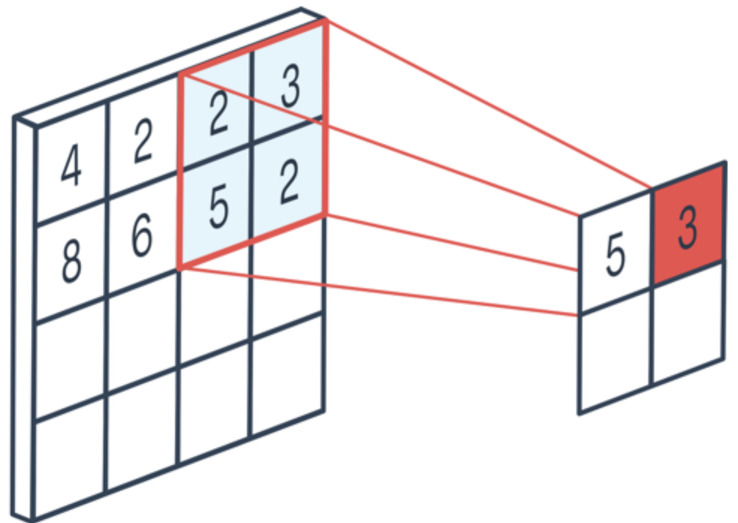

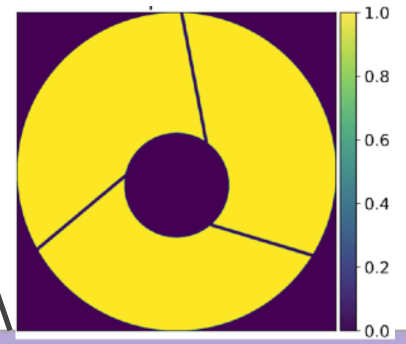

Obscurations

WFE
Parametric part

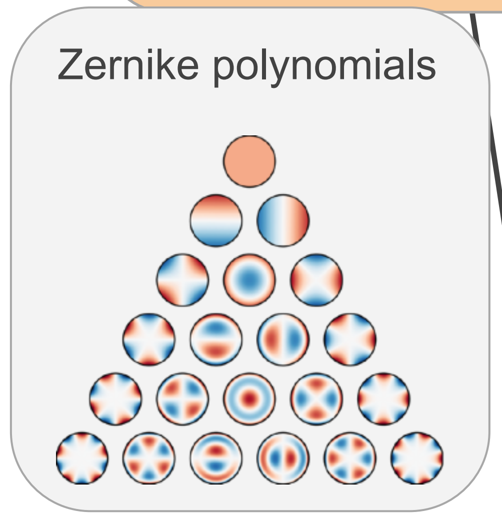

WFE
Non-parametric part

Wavefront PSF model

Downsampling operator

T. Liaudat, J.-L. Starck, M. Kilbinger, P.-A. Frugier, "Rethinking the modeling of the instrumental response of telescopes with a differentiable optical model", Inverse Problems, 39, 3, 2023.

Euclid Point Spread Function Field

Pixel errors with respect to noiseless ground truth polychromatic PSF at Euclid resolution.

Model	Train stars RMSE	Test stars RMSE
Parametric	1.1087e-03 (14.16%)	1.0950e-03 (14.45%)
WF-RCA	2.4031e-04 (3.07%)	2.7927e-04 (3.68%)

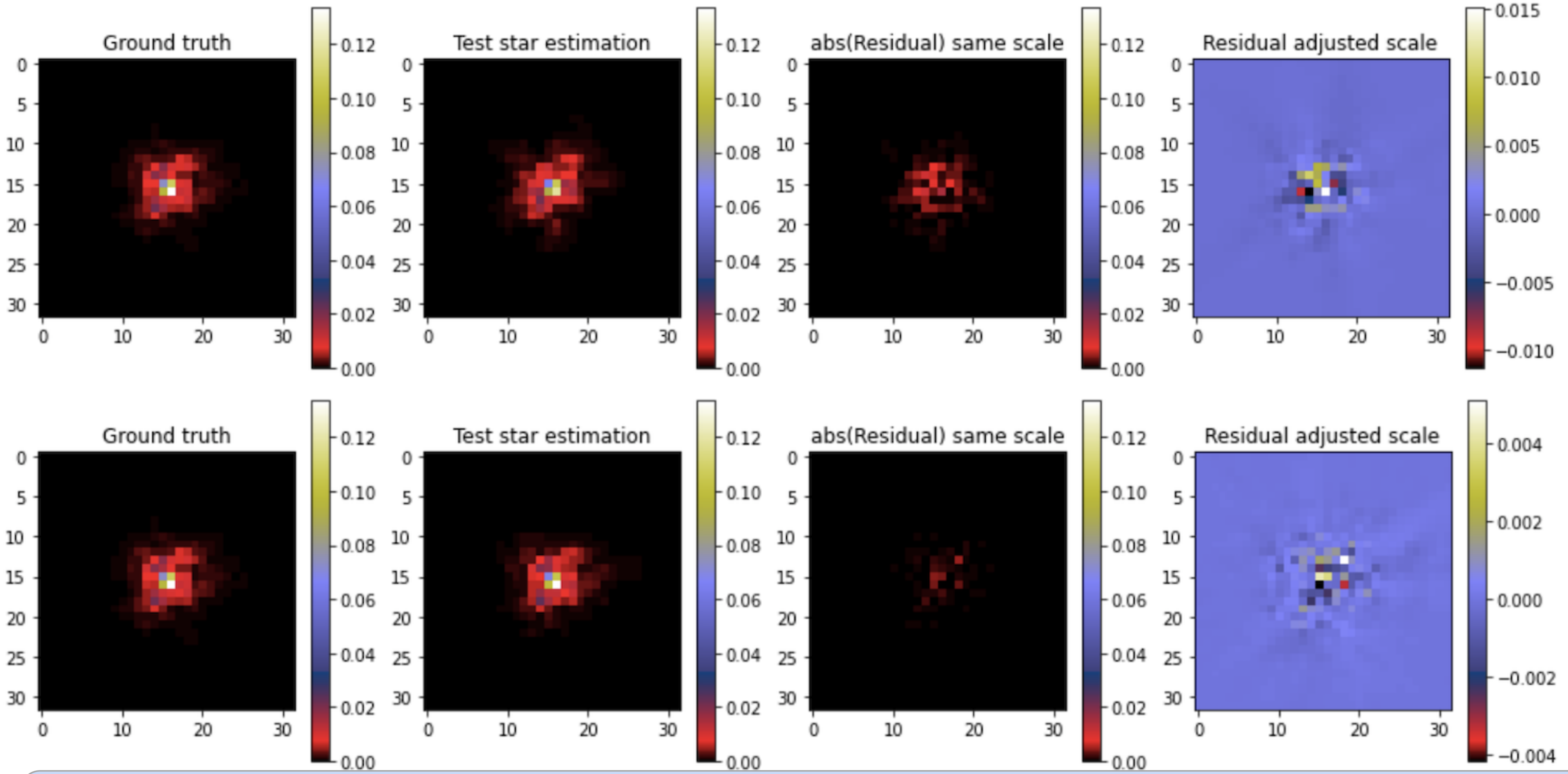

→ WF-RCA improves by a factor of 4 the RMSE compared to the parametric model which uses the ground truth underlying model.

➡Part 1: Introduction

➡Part 2: Ground Based Telescope PSF

➡Part 3: Space Telescope PSF

➡**Part 4: Joint Rubin-Euclid Deconvolution**

Motivations

-**Euclid:**
- High resolution: good for galaxies detection and shape measurement.
- Need extra colors for redshift estimation.

Rubin:
- More bands
- Lower resolution (blending of galaxies, etc)

Ideally, we would like to have a **Joint Euclid-Rubin (JEUBIN Catalog),** using both **Euclid resolution** and **Rubin colours.**

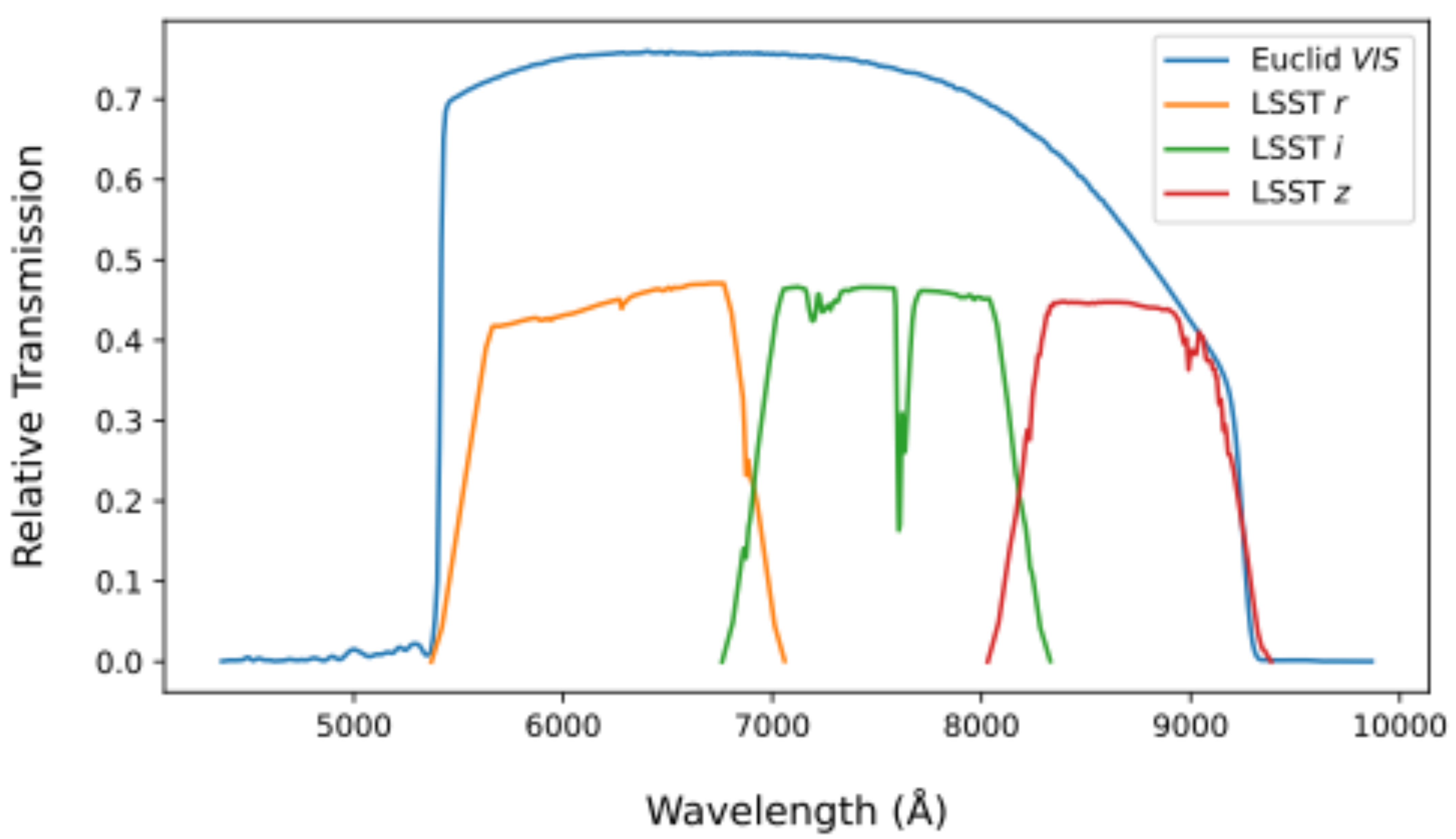

$$\mathbf{x}_{euc} = \alpha_r \mathbf{x}_r + \alpha_i \mathbf{x}_i + \alpha_z \mathbf{x}_z$$

Fractional flux contributions

$$\alpha_r,\ \alpha_i,\ \alpha_z \in \mathbb{R}^n$$

U. Akhaury, P. Jablonka, F. Courbin, and J.-L. Starck, "**Joint multi-band deconvolution for Euclid and Rubin images**", A&A, 697, id.A136, 2025.

Euclid-Rubin Image Relation

Rubin Images

$$\mathbf{y}_r = \mathbf{h}_r * \mathbf{x}_r^t + \eta_r$$

$$\mathbf{y}_i = \mathbf{h}_i * \mathbf{x}_i^t + \eta_i$$

$$\mathbf{y}_z = \mathbf{h}_z * \mathbf{x}_z^t + \eta_z$$

Euclid Image

$$\mathbf{y}_{euc} = \mathbf{h}_{euc} * \mathbf{x}_{euc}^t + \eta_{euc}$$

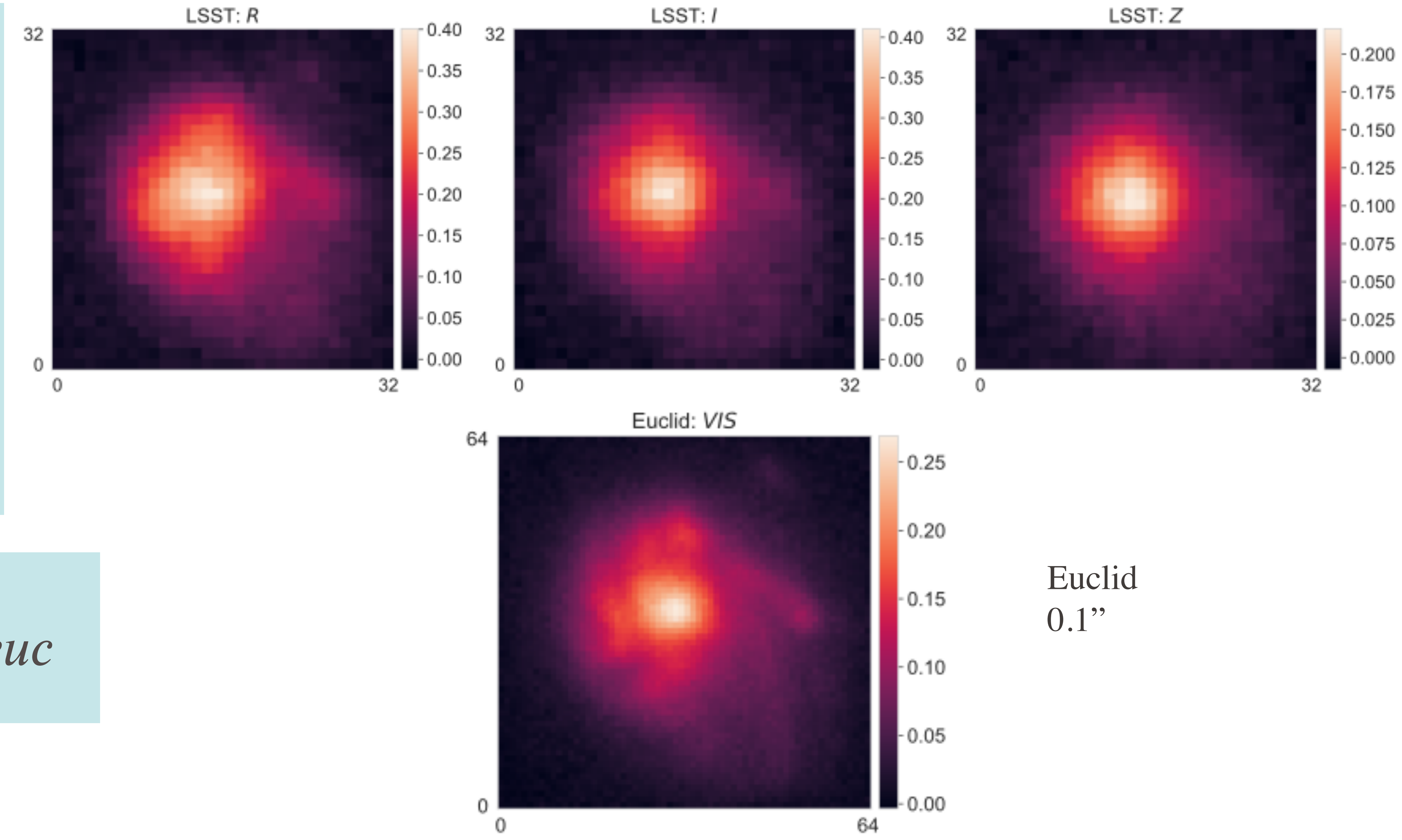

Rubin
0.2”

Euclid
0.1”

$$\boxed{\mathbf{x}_{euc}^t = \alpha_r \mathbf{x}_r^t + \alpha_i \mathbf{x}_i^t + \alpha_z \mathbf{x}_z^t}$$

The Rubin-Euclid Deconvoluton Problem

$$L_r(\mathbf{x}_r) = \frac{1}{2}\left\| \frac{\mathbf{h}_r * \mathbf{x}_r - \mathbf{y}_r}{\sigma_r} \right\|_F^2 + \lambda_{constr} \left\| \frac{\mathbf{h}_{euc} * \sum_c \alpha_c \mathbf{x}_c - \mathbf{y}_{euc}}{\sigma_{euc}} \right\|_F^2$$

$$L_i(\mathbf{x}_i) = \frac{1}{2}\left\| \frac{\mathbf{h}_i * \mathbf{x}_i - \mathbf{y}_i}{\sigma_i} \right\|_F^2 + \lambda_{constr} \left\| \frac{\mathbf{h}_{euc} * \sum_c \alpha_c \mathbf{x}_c - \mathbf{y}_{euc}}{\sigma_{euc}} \right\|_F^2$$

$$L_z(\mathbf{x}_z) = \frac{1}{2}\left\| \frac{\mathbf{h}_z * \mathbf{x}_z - \mathbf{y}_z}{\sigma_z} \right\|_F^2 + \lambda_{constr} \left\| \frac{\mathbf{h}_{euc} * \sum_c \alpha_c \mathbf{x}_c - \mathbf{y}_{euc}}{\sigma_{euc}} \right\|_F^2$$

$$\boxed{\min_{x_r, x_i, x_z} L_r(x_r) + L_i(x_i) + L_z(x_z)}$$

Optimisation

Loss Functions iteratively minimized using Gradient Descent

$$\mathbf{x}_{\{r,i,z\}}^{[k+1]} = \mathbf{x}_{\{r,i,z\}}^{[k]} - \beta_{\{r,i,z\}} \nabla L_{\{r,i,z\}}\left(\mathbf{x}_{\{r,i,z\}}^{[k]}\right)$$

Step Sizes

$$\beta_r,\ \beta_i,\ \beta_z \in \mathbb{R}^n$$

Gradients of the Loss Functions

$$\nabla L_r(\mathbf{x}_r) = \frac{\mathbf{h}_r^\top * (\mathbf{h}_r * \mathbf{x}_r - \mathbf{y}_r)}{\|\sigma_r\|_F^2} + 2\lambda_{constr}\alpha_r \mathbf{h}_{euc}^\top * \left[\frac{\mathbf{h}_{euc} * \sum_c \alpha_c \mathbf{x}_c - \mathbf{y}_{euc}}{\|\sigma_{euc}\|_F^2}\right]$$

$$\nabla L_i(\mathbf{x}_i) = \frac{\mathbf{h}_i^\top * (\mathbf{h}_i * \mathbf{x}_i - \mathbf{y}_i)}{\|\sigma_i\|_F^2} + 2\lambda_{constr}\alpha_i \mathbf{h}_{euc}^\top * \left[\frac{\mathbf{h}_{euc} * \sum_c \alpha_c \mathbf{x}_c - \mathbf{y}_{euc}}{\|\sigma_{euc}\|_F^2}\right]$$

$$\nabla L_z(\mathbf{x}_z) = \frac{\mathbf{h}_z^\top * (\mathbf{h}_z * \mathbf{x}_z - \mathbf{y}_z)}{\|\sigma_z\|_F^2} + 2\lambda_{constr}\alpha_z \mathbf{h}_{euc}^\top * \left[\frac{\mathbf{h}_{euc} * \sum_c \alpha_c \mathbf{x}_c - \mathbf{y}_{euc}}{\|\sigma_{euc}\|_F^2}\right]$$

Convergence Guarantee & Optimal step size

A function's gradient is Lipschitz continuous if :

$$\left\| \nabla f(\mathbf{x}') - \nabla f(\mathbf{x}) \right\| \le C \left\| \mathbf{x}' - \mathbf{x} \right\|$$

where C is the Lipschitz constant

In our case:

$$\left\| \nabla L_{\{r,i,z\}}\left(\mathbf{x}'_{\{r,i,z\}}\right) - \nabla L_{\{r,i,z\}}\left(\mathbf{x}_{\{r,i,z\}}\right) \right\| \le C_{\{r,i,z\}} \left\| \mathbf{x}'_{\{r,i,z\}} - \mathbf{x}_{\{r,i,z\}} \right\|$$

Substituting the individual loss functions, we get:

$$C_{\{r,i,z\}} \ge \frac{\mathbf{h}^{\top}_{\{r,i,z\}} * \mathbf{h}_{\{r,i,z\}}}{\left\| \sigma_{\{r,i,z\}} \right\|_F^2} + \frac{2\lambda_{constr} \alpha^2_{\{r,i,z\}} \mathbf{h}^{\top}_{euc} * \mathbf{h}_{euc}}{\left\| \sigma_{euc} \right\|_F^2}$$

The Optimal Condition for Convergence

$$\beta_{\{r,i,z\}} \le \frac{1}{C_{\{r,i,z\}}}$$

Hence, we choose

$$\beta_{\{r,i,z\}} = \frac{1}{\left(1 + 10^{-5}\right) C_{\{r,i,z\}}}$$

Simulations

Ground Truth Images

- HST cutouts of 128 × 128 pixels from GOODS-N and GOODS-S in the following filters:
  - F606W
  - F775W
  - F850LP

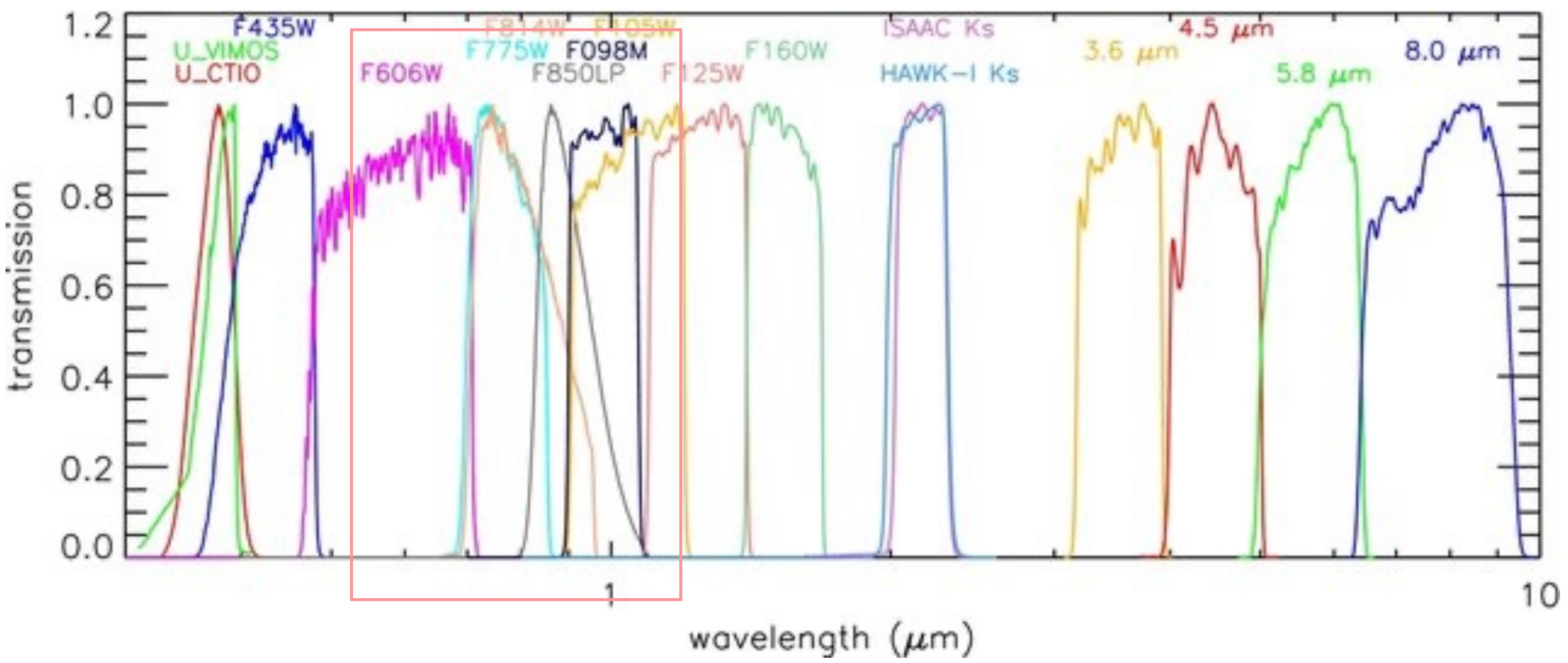

Noisy Simulations

- Calculated fractional flux contributions $(\alpha_r, \alpha_i, \alpha_z)$ from filter curves
- Convolved ground-truth images with corresponding PSFs
- Added White Gaussian noise such that
  - *Rubin*-simulated images have a signal-to-noise (S/N) ratio ranging between 12 and 28
  - *Euclid*-simulated images have a signal-to-noise (S/N) ratio ranging between 20 and 45

$$\mathbf{y}_r = \mathbf{h}_r * \mathbf{x}_r^t + \eta_r$$
$$\mathbf{y}_i = \mathbf{h}_i * \mathbf{x}_i^t + \eta_i$$
$$\mathbf{y}_z = \mathbf{h}_z * \mathbf{x}_z^t + \eta_z$$

$$\mathbf{x}_{euc}^t = \alpha_r \mathbf{x}_r^t + \alpha_i \mathbf{x}_i^t + \alpha_z \mathbf{x}_z^t$$
$$\mathbf{y}_{euc} = \mathbf{h}_{euc} * \mathbf{x}_{euc}^t + \eta_{euc}$$

Experiment 1

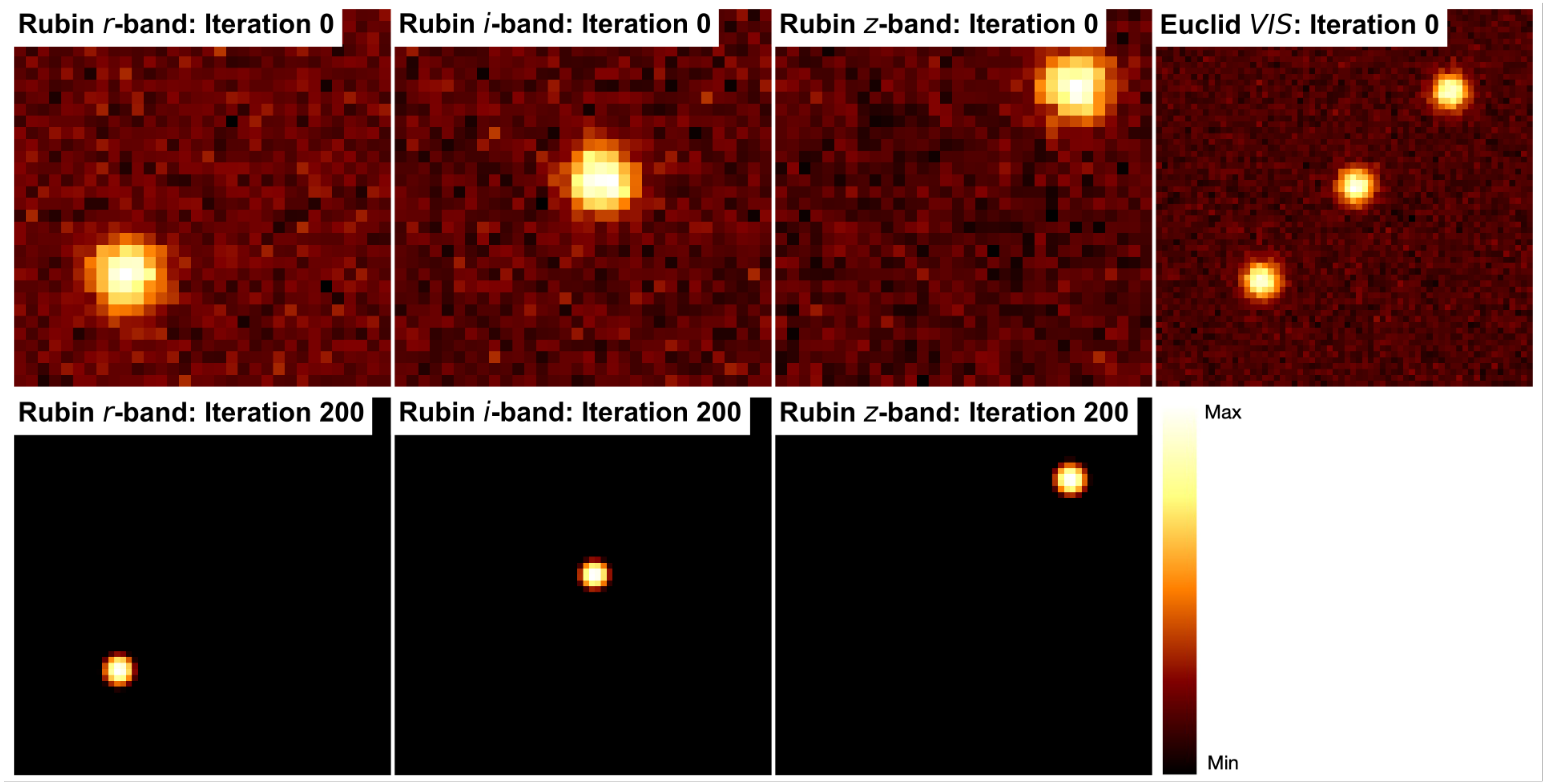

- Assume 3 separately placed Gaussians in each channel (corresponding to LSST channels)
- The joint image (Euclid) is a linear sum of these channels
- No Flux Leakage from one channel to another

Experiment 2

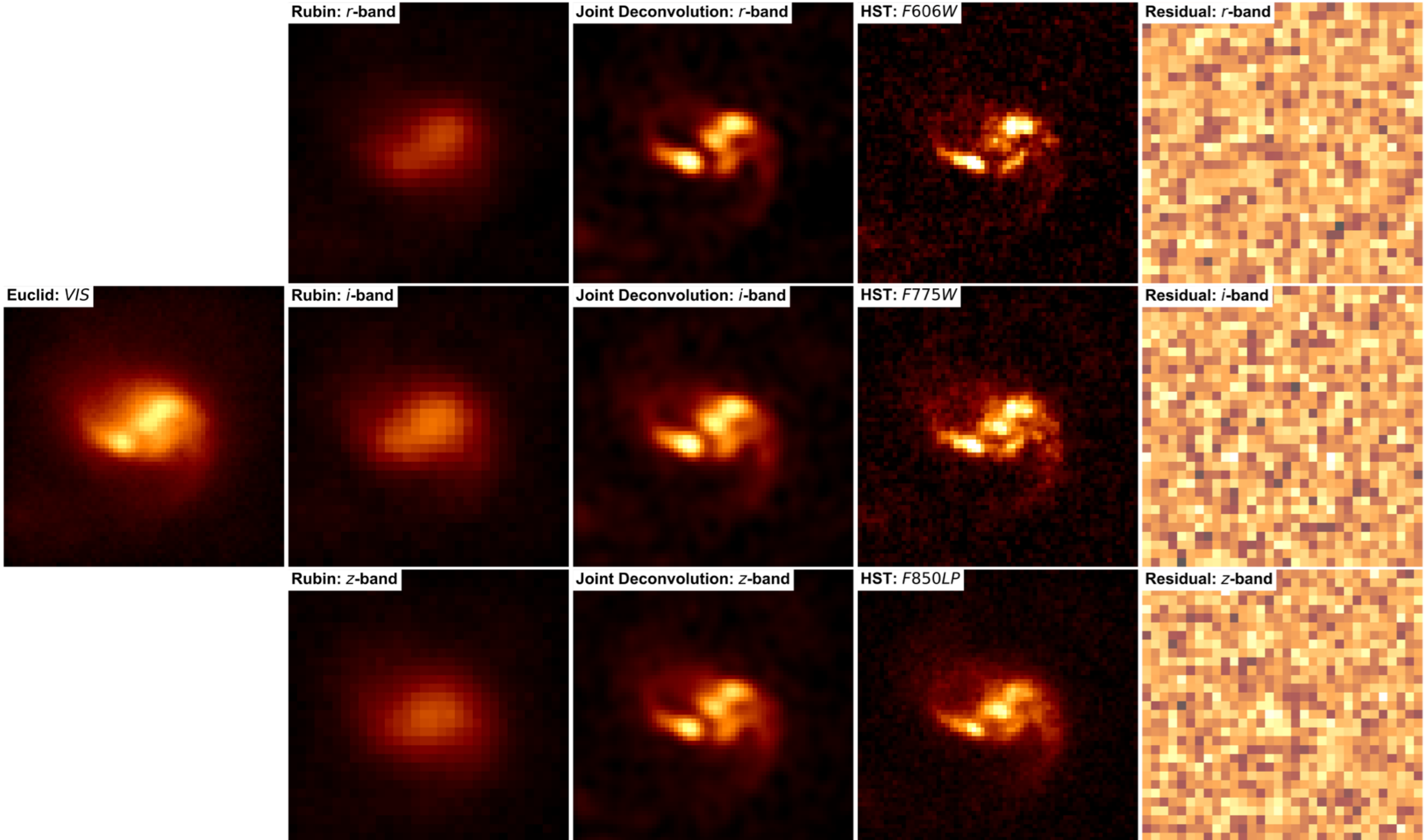

Convergence

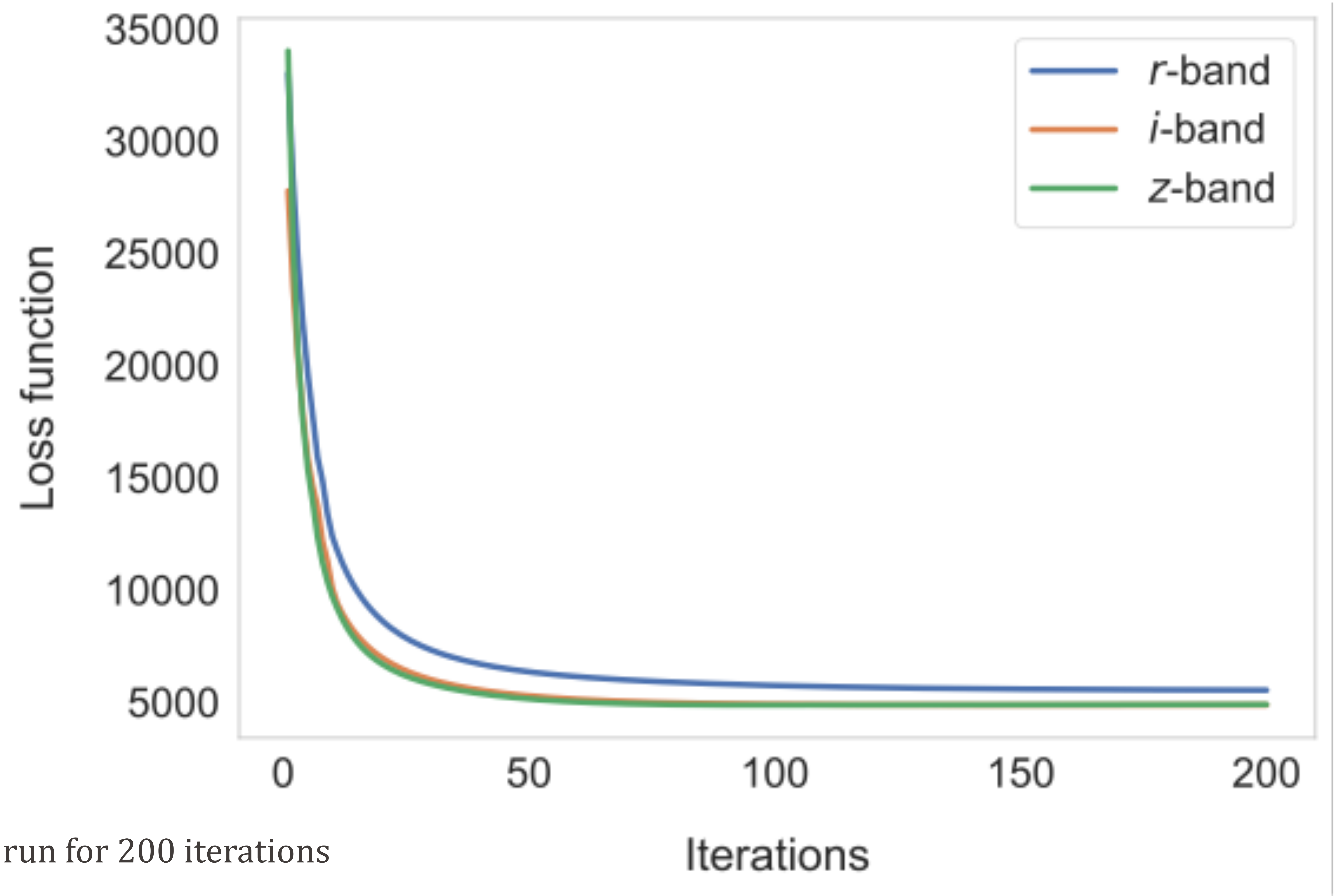

- Algorithm run for 200 iterations
- Convergence within 50-100 iterations

Post-Processing Denoising

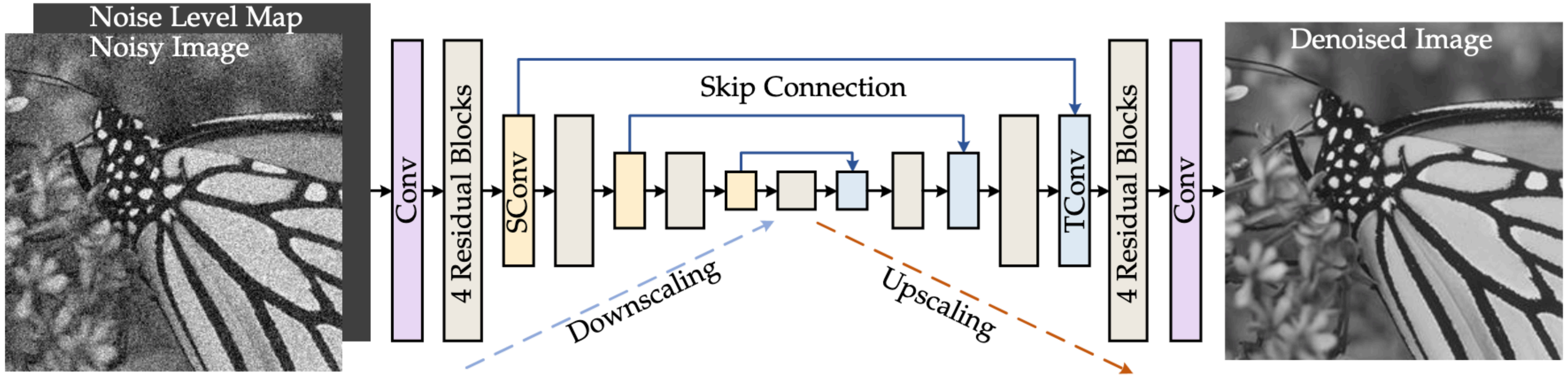

Plug-and-Play Image Restoration with Deep Denoiser Prior, *Zhang et al., 2021*

NMSE	r-band	i-band	z-band
Pre-denoising	0.059	0.041	0.053
Post-denoising	0.058	0.038	0.038
% improvement	1.69%	7.32%	28.3%

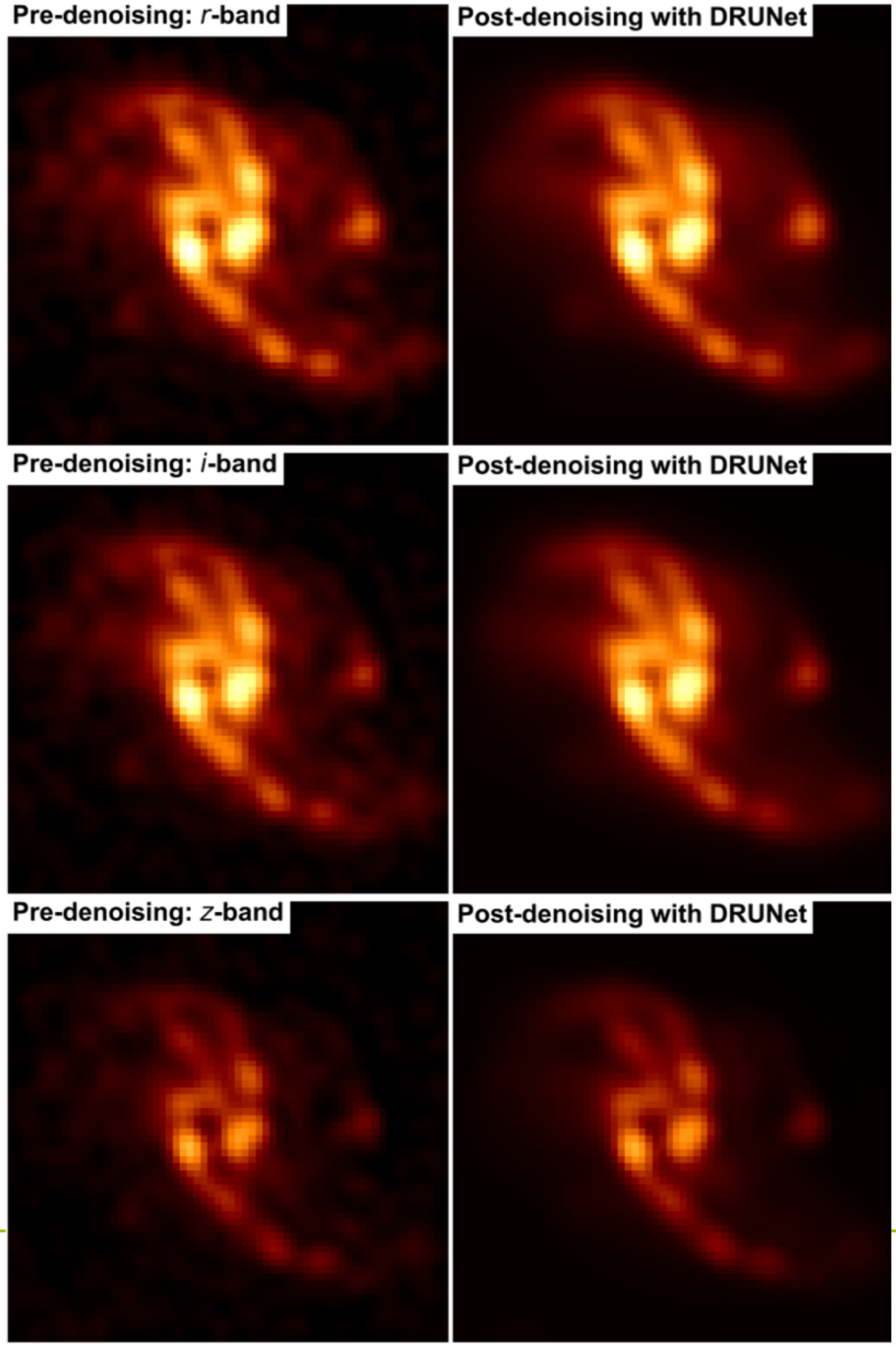

Flux Recovery

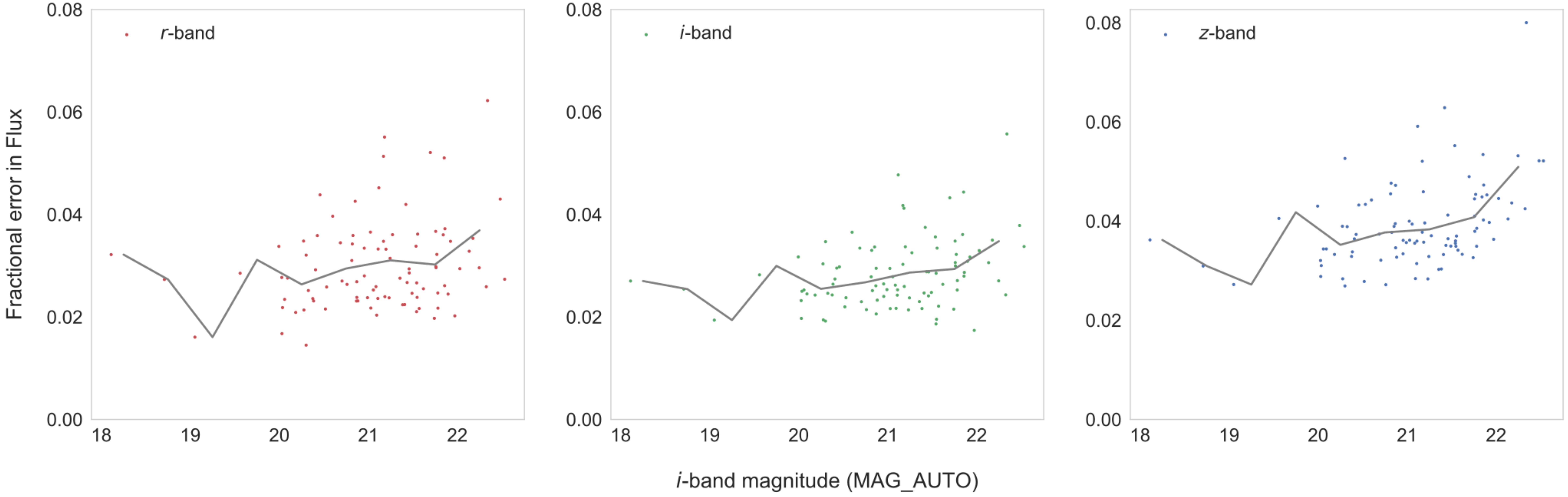

S/N before deconvolution

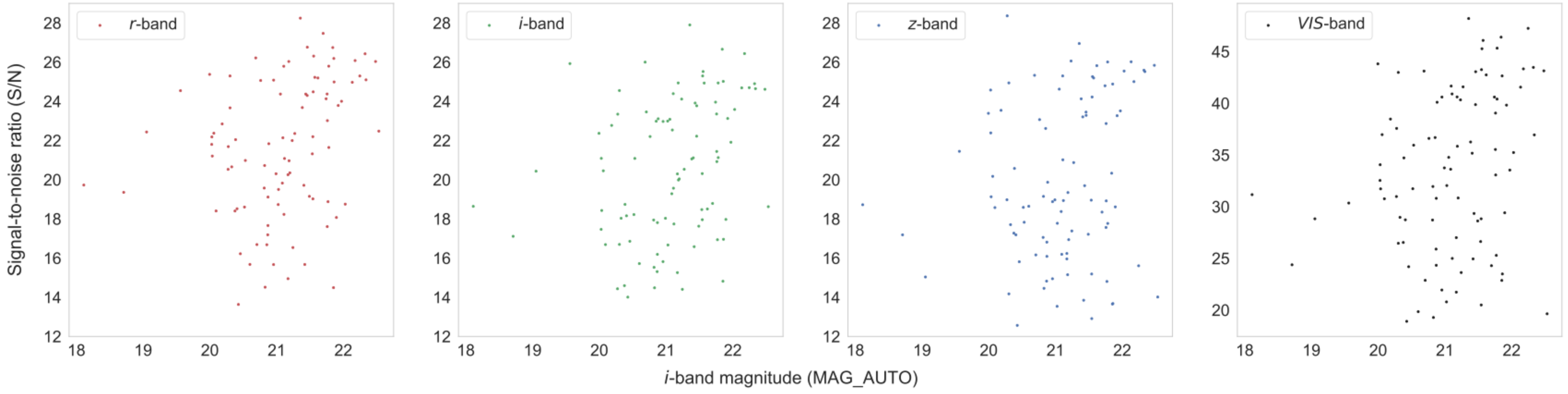

S/N after deconvolution

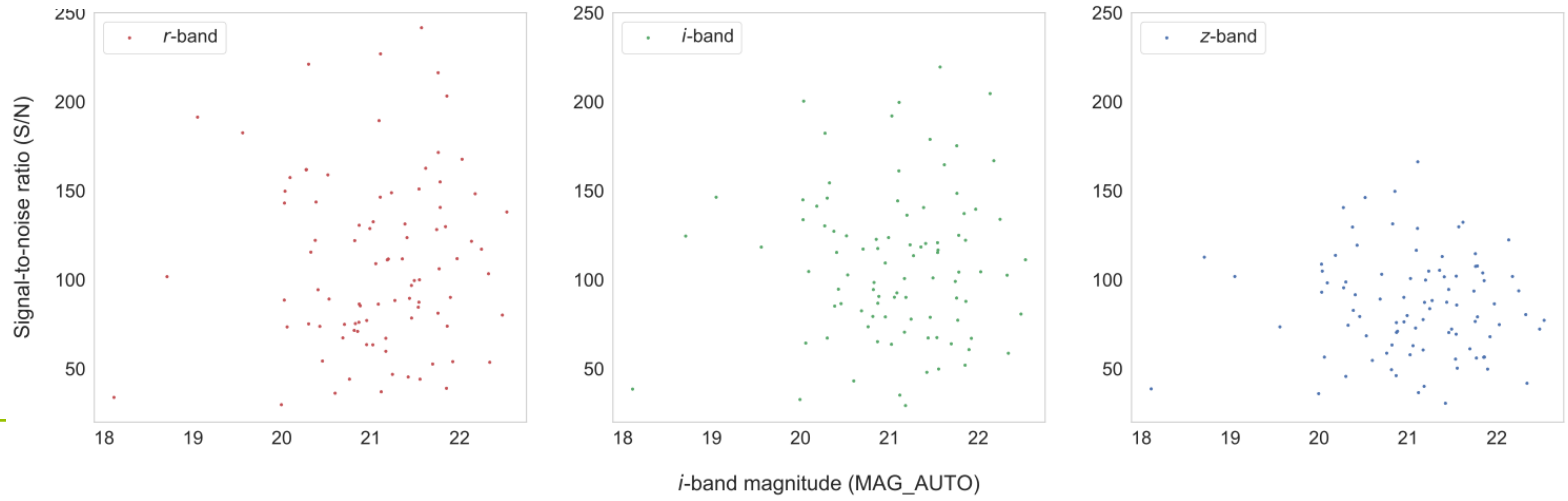

Experiment on CFHT Images (Perseus Cluster) / Euclid ERO Image

Utsav Akhau

•U. Akhaury, P. Jablonka, F. Courbin and **J.-L. Starck**, "Joint multi-band deconvolution for Euclid and Vera C. Rubin images", A&A, 697, id.A136, 2025

Deconvolution of Rubin/lSST images using Euclid VIS information

Experiment: Three bands from **CHFT Megacam** instrument and its corresponding **Euclid VIS image**

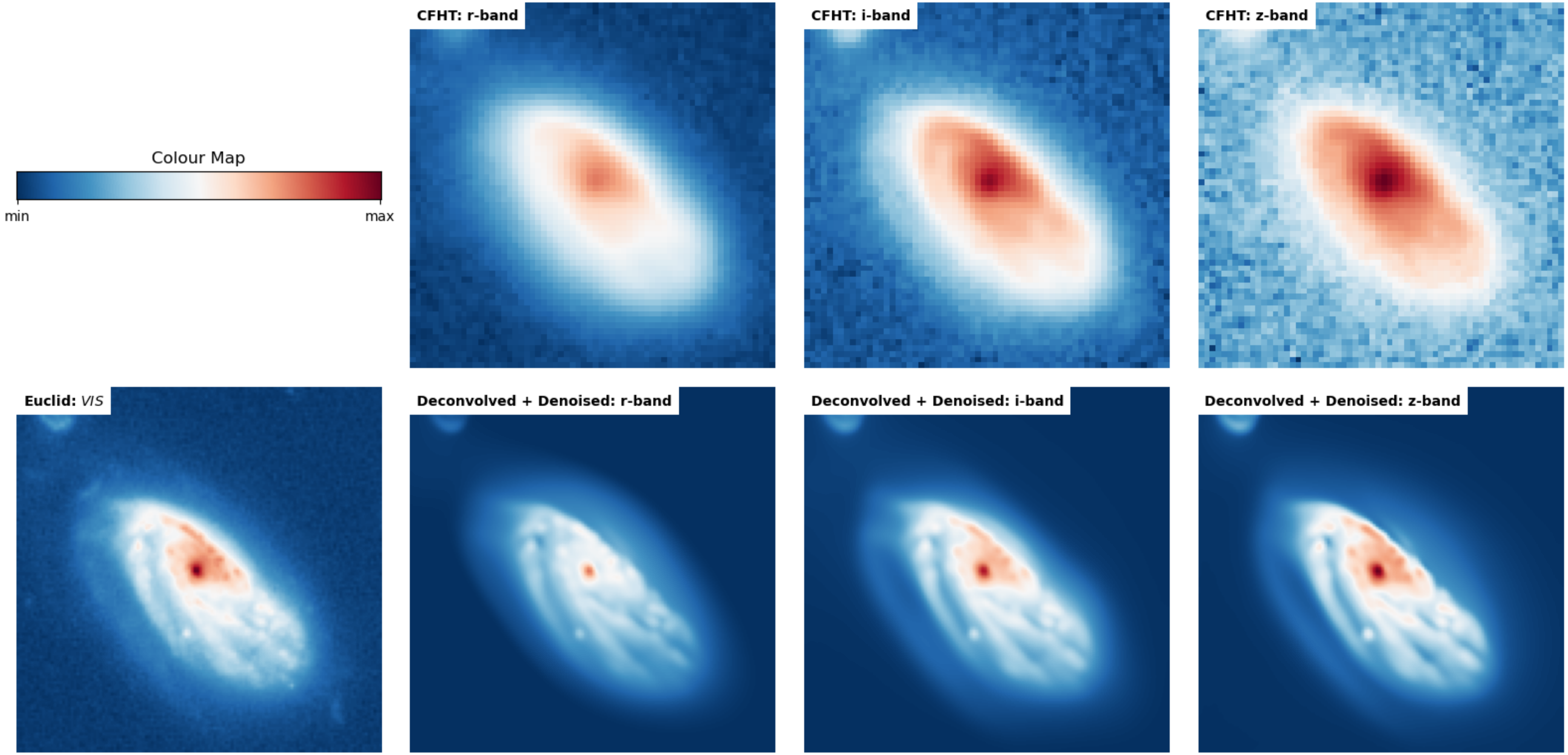

Computation time: 5s on a single CPU.

Sanity check 1

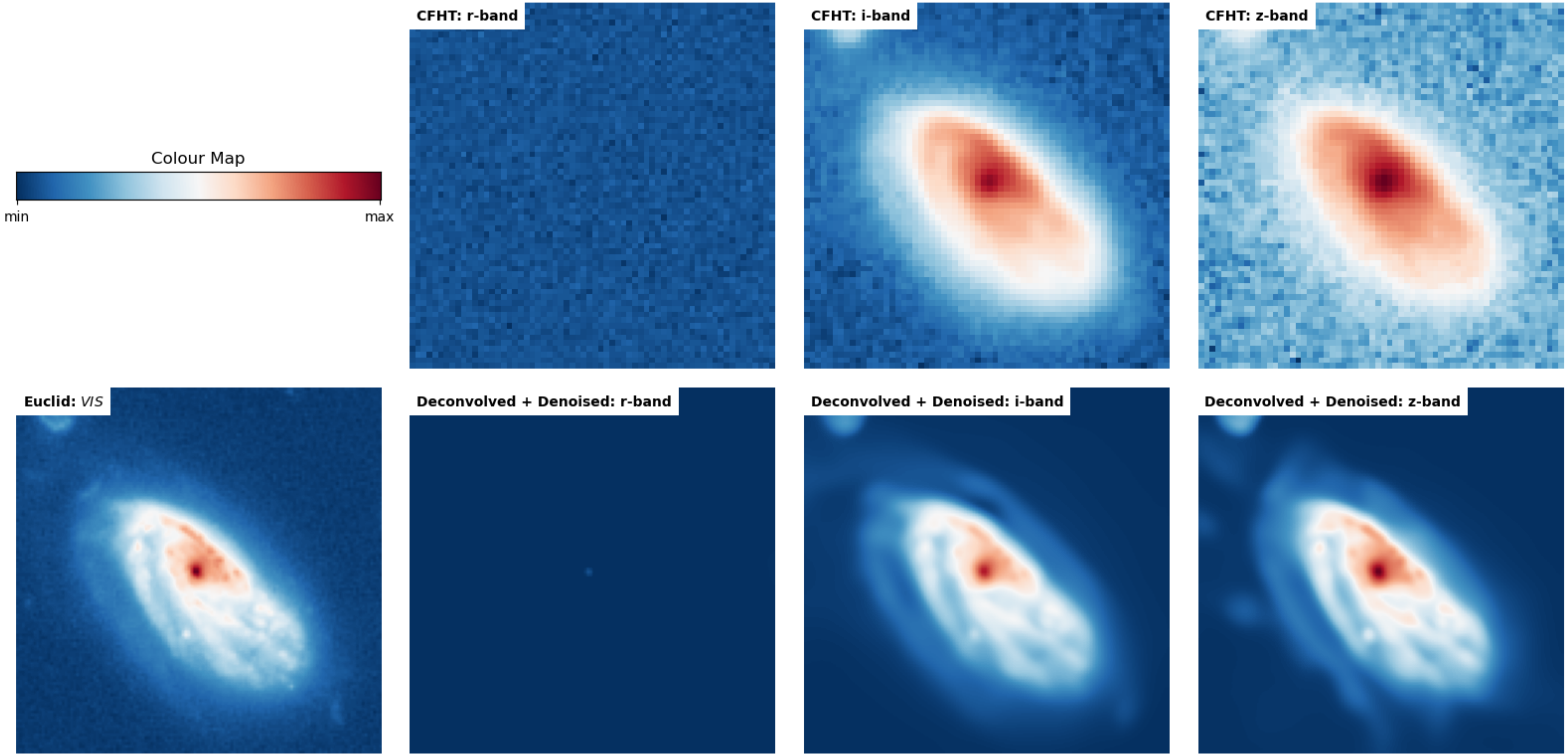

Sanity check 2

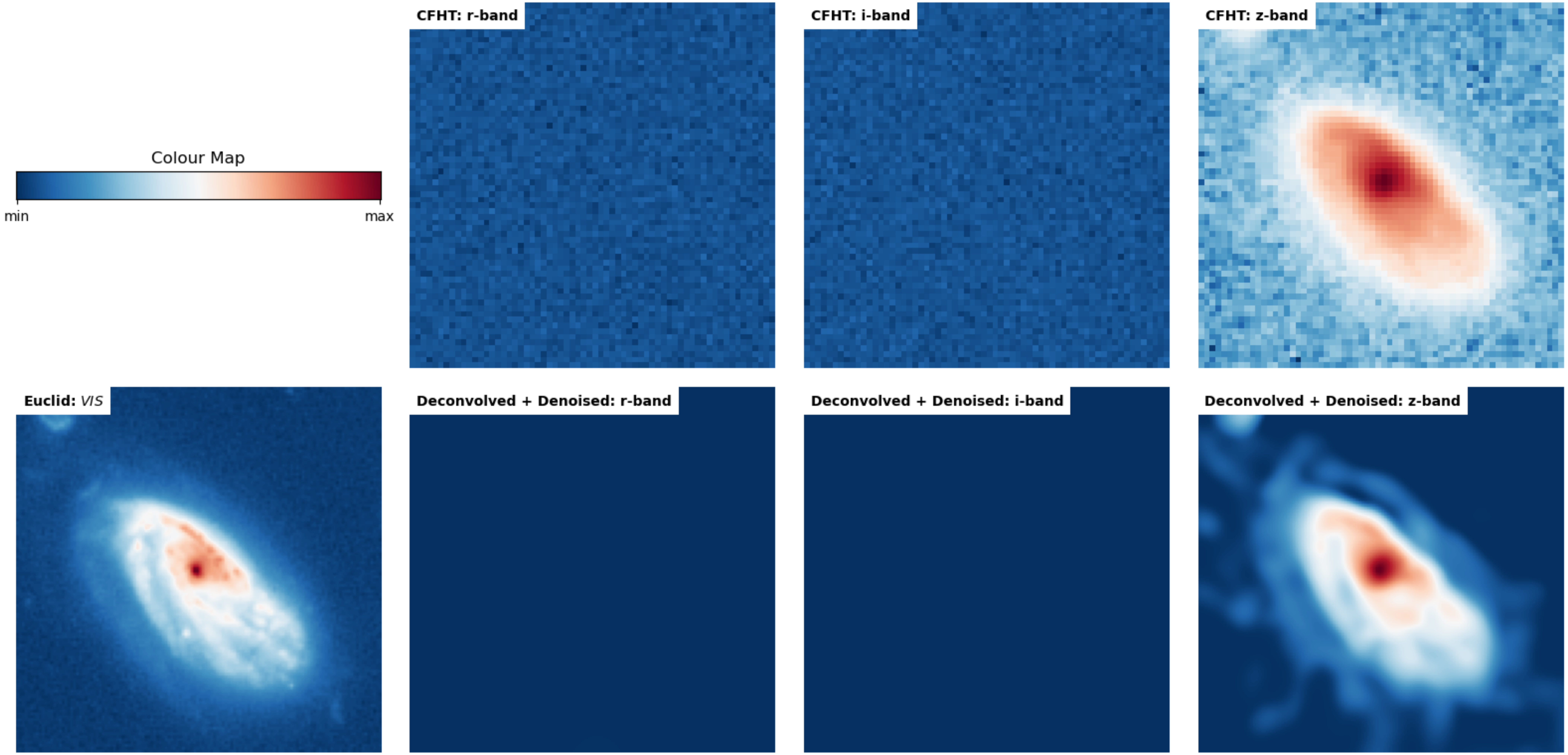

Sanity check 3

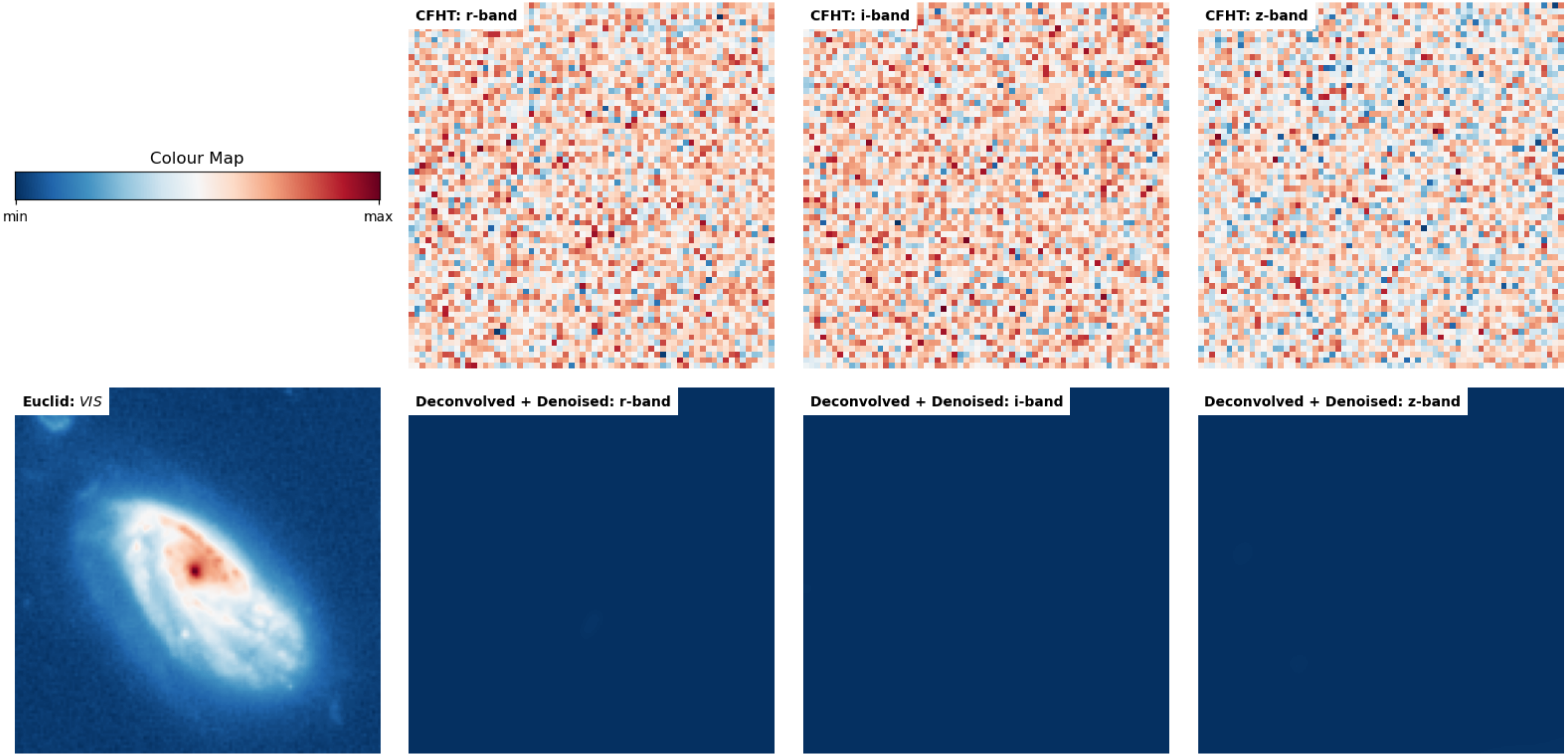

H. Leterme

J. Fadili

Conformalized quantile regression (CQR)

- Y. Romano, E. Patterson, and E. Candès. NeurIPS, 2019
- H. Leterme, J. Fadili and J.-L. Starck,"**Distribution-free uncertainty quantification for inverse problems**: application to weak lensing mass mapping", A&A, 694, id.A267, ArXiv:2410.088312024, 2025.

Goal: given $\boldsymbol{\gamma}$, estimate $\hat{\boldsymbol{\kappa}}^-$ and $\hat{\boldsymbol{\kappa}}^+$ such that

$$\mathbb{E}\left[L\left(\boldsymbol{\kappa}, \hat{\boldsymbol{\kappa}}^-, \hat{\boldsymbol{\kappa}}^+\right)\right] \leq \alpha.$$

E.g., $g_\lambda\left(\hat{r}\right) = \hat{r} + \lambda$

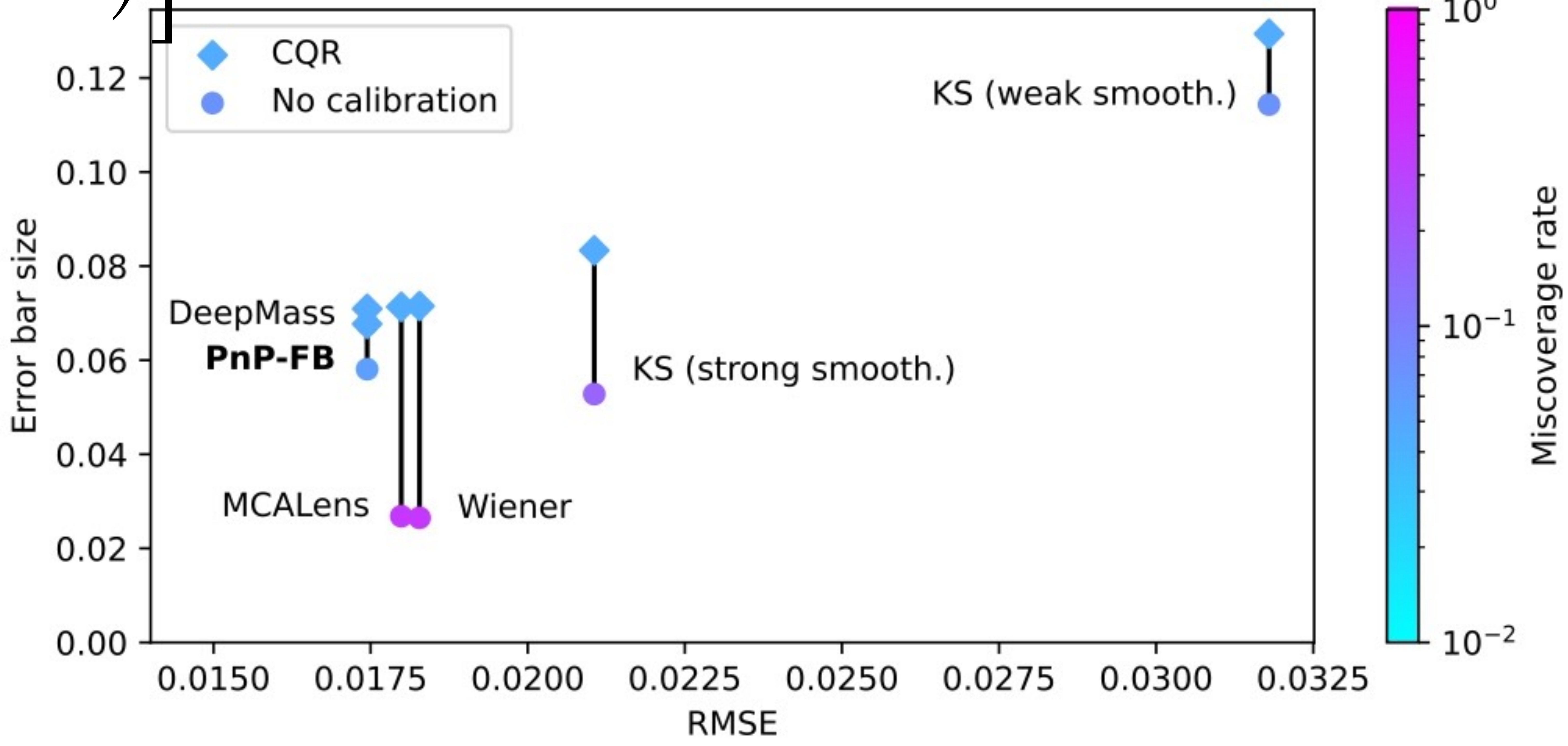

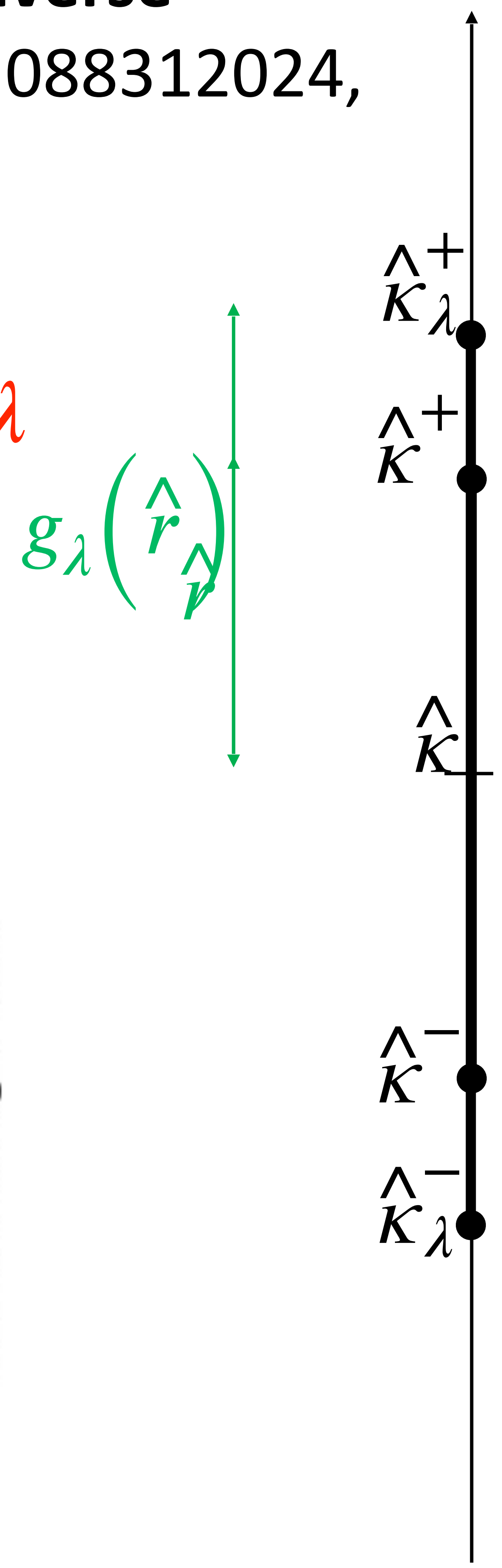

Conclusions

U. Akhaury, P. Jablonka, F. Courbin, and J.-L. Starck, "**Joint multi-band deconvolution for Euclid and Rubin images**", A&A, 697, id.A136, 2025.

✓ **A new method for deconvolving Rubin images using Euclid information**

➡ **Very nice results : resolution, flux, SNR …**

➡ **Deep Learning post-processing**

➡ **Experiment on real data (CFHT/Euclid):** could be improved with a PSF estimations for both CFHT and Euclid.

✓ **Perspectives:**

➡ **Include the Euclid in flight PSF model**

➡ **Use MCCD method for Rubin PSF and WaveDiff for Euclid PSF**

➡ **Use more efficient optimisation techniques (pre-conditioner, proximal methods)**

➡ **Estimate uncertainties (Conformalized Quantile Regression)**